Chemical composition of Earth's primitive mantle and its variance:

1. Method and results

Tanya Lyubetskaya[1] and Jun Korenaga[1]

[1]   We present a new statistical method to construct a model for the chemical composition of Earth's primitive mantle along with its variance. Earth's primitive mantle is located on the melting trend exhibited by the global compilation of mantle peridotites, using cosmochemical constraints on the relative abundances of refractory lithophile elements (RLE). This so-called pyrolite approach involves the least amount of assumptions, thereby being probably most satisfactory compared to other approaches. Its previous implementations, however, suffer from questionable statistical treatment of noisy geochemical data, leaving the uncertainty of model composition poorly quantified. In order to properly take into account how scatters in peridotite data affect this geochemical inference, we combine the following statistical techniques: (1) modeling a nonlinear melting trend in the multidimensional compositional space through the principal component analysis, (2) determining the primitive mantle composition on the melting trend by simultaneously imposing all of cosmochemical constraints with least squares, and (3) mapping scatters in original data into the variance of the final model through the bootstrap resampling technique. Whereas our model is similar to previous models in terms of Mg, Si, and Fe abundances, the RLE contents are at $\sim 2.16 \pm 0.37$ times the CI chondrite concentration, which is lower than most of previous estimates. The new model is depleted by >20% in a number of incompatible elements including heat-producing elements, U, Th, and K, and this depleted nature is further amplified (up to 60%) in terms of predicted composition for the present-day mantle.

Citation: Lyubetskaya, T., and J. Korenaga (2007), Chemical composition of Earth's primitive mantle and its variance: 1. Method and results, *J. Geophys. Res.*, *112*, B03211, doi:10.1029/2005JB004223.

1. Introduction

[2]   The accurate knowledge of the chemical composition of the mantle is a foundation for many geophysical and geochemical models. It can serve as a strong guideline as well as constraints when we try to quantify Earth accretion processes and subsequent global differentiation processes such as core segregation and crust-mantle differentiation. Also, the present-day concentrations of heat-producing elements in the bulk silicate Earth are essential for calculating Earth's thermal budget and evolution.

[3]   As we cannot directly measure the composition of the entire Earth, however, we must rely on some kind of geochemical inference. One approach to determine Earth's composition utilizes cosmochemical data, based on the assumption that the sun, planets and meteorites all accreted from the solar nebula. Chondritic meteorites are considered the most representative samples of the nebular material. They did not experience melting and igneous differentia-

tion, and their abundances of nonvolatile elements are close to those in the solar photosphere [e.g., *Palme and Jones*, 2003; *Scott and Krot*, 2003]. In this approach, therefore, Earth is identified with a particular class of chondritic meteorites, or with a mixture of some classes of chondrites, and mixing ratios are adjusted to satisfy such constraints as core size, heat flow, and terrestrial ratios of certain elements [e.g., *Morgan and Anders*, 1980; *Javoy*, 1995]. Because Earth is known to be highly depleted in volatile elements [e.g., *Gast*, 1960; *Wasserburg et al.*, 1964], however, this approach has to involve a number of assumptions on accretion and fractionation processes to reconstruct the chemical composition of bulk silicate Earth from that of chondritic meteorites [e.g., *Wänke*, 1981; *Wänke and Dreibus*, 1988; *Allègre et al.*, 2001].

[4]   An alternative approach, based on the analysis of terrestrial samples, can directly yield an estimate on the chemical composition of primitive mantle. "Primitive mantle" (PM) and "bulk silicate Earth" (BSE) are synonymous referring to the chemical composition of mantle after core segregation but before the extraction of continental crust. This approach based on terrestrial samples is more satisfactory compared to the cosmochemical approach, since it does not require assumptions about the composition of materials

[1]Department of Geology and Geophysics, Yale University, New Haven, Connecticut, USA.

from which Earth accreted, or fractionation processes in the solar nebula. Not surprisingly, the de facto reference model of Earth's chemical composition [*McDonough and Sun*, 1995] is based on this petrological approach.

[5] The petrological approach utilizes compositional trends in upper mantle peridotites [*Hart and Zindler*, 1986; *McDonough and Sun*, 1995; *Palme and O'Neill*, 2003]. The observed range of mantle peridotite compositions is believed to result mainly from previous melt depletion and fertilization processes on primitive mantle. Major trends in peridotite data are thus interpreted as melting trends, and the primitive mantle composition is located on these trends using some cosmochemical constraints, which are usually chondritic values for the relative abundances of refractory lithophile elements (RLE). Lithophile elements are those which are not affected by core segregation and stay in the silicate mantle. Refractory elements are characterized by very high condensation temperature (>1400 K at 10^{-4} atm) and therefore are first to condensate during cooling of the solar nebula [*Davis and Richter*, 2003; *Lodders*, 2003]. Presumably, they do not suffer any preaccretional differentiation and become fractionated only after they are in a planet. Refractory lithophile elements, such as Ca, Al, Ti, rare earth elements (REE), U, and Th, occur in roughly constant proportions in different classes of chondrites and also in the solar photosphere [*Wasson and Kallemeyn*, 1988; *Lodders and Fegley*, 1998]. It is thus reasonable to assume that the ratios of these elements in the bulk silicate Earth should be (at least approximately) equal to those in chondritic meteorites. Therefore the petrological approach is not entirely based on terrestrial data alone, but it incorporates only the most robust cosmochemical argument.

[6] However, the petrological approach has a number of intrinsic problems, including the nonuniqueness of (either theoretical or empirical) melting models fitted to compositional trends, very large scatters of peridotite data, and the difficulty of imposing multiple cosmochemical constraints. As a result, the statistical treatment of geochemical data in previous studies is often questionable, and model uncertainty is poorly quantified. A recent study by *Palme and O'Neill* [2003] presents a mass balance approach for calculating the primitive mantle composition, which is believed to allow them to assign reasonable model uncertainty. However, this approach requires an additional assumption about the primitive mantle Mg # (defined as molar Mg/(Mg + Fe) × 100). The resultant PM model is highly sensitive to this assumed Mg #, and the reasonable range of primitive Mg # inferred from fertile mantle peridotites results in a very large uncertainty of the PM model (see section 5.1 for detailed discussion). As the chemical composition of Earth's mantle plays a critical role in a number of geochemical and geophysical models, it is important to establish a composition model with its uncertainty firmly quantified. To this end, we present a new statistical method to construct a model for the chemical composition of Earth's mantle along with its variance. To resolve the aforementioned intrinsic difficulties we combine the following three statistical techniques: (1) modeling a nonlinear melting trend in the multidimensional compositional space through the principal component analysis (PCA), (2) determining the most primitive (i.e., most chondritic) mantle composition on the melting trend by simultaneously imposing all of chondritic constraints with least squares, and (3) mapping scatters in original data into the variance of the final composition model through the Monte Carlo bootstrap resampling method.

[7] The major limitation of the petrological approach to construct the bulk Earth composition is the use of mantle peridotite samples, which come from depths of less than 300 km. Any model of the primitive mantle based on petrological data thus requires the assumption of global-scale homogeneity of Earth's mantle. Otherwise, the resultant primitive mantle model would only reflect the composition of the upper mantle. Geophysical observations of subducting slabs penetrating the 660 km discontinuity and deep mantle plumes [*van der Hilst et al.*, 1997; *Fukao et al.*, 2001; *Montelli et al.*, 2004] along with dynamical constraints derived from numerical modeling of Earth's geoid [e.g., *Hager et al.*, 1985] constitute a strong support for the whole mantle convection model. However, a number of geochemical arguments suggest that there must be at least one additional, volumetrically significant mantle reservoir that has remained separate from the rest of the mantle for geologically significant amount of time [e.g., *Allègre et al.*, 1996; *Turcotte et al.*, 2001]. These arguments, most of which rest on the presumed BSE composition, will be critically reviewed in our companion paper in light of the new composition model derived here.

[8] The full account of the new method, with detailed discussion on the problems of previous studies, is given in section 3. The resulting new composition model for Earth's mantle is presented in section 4. Its bearing on the structure and evolution of the mantle will be fully explored in the companion paper. We begin with the description of geochemical and cosmochemical data used in our study.

2. Data

2.1. Terrestrial Data

[9] The compositional data of mantle peridotites, kindly provided by W.F. McDonough, contain more than 800 spinel lherzolites including both xenoliths and massif peridotites. The following selection criteria, similar to those adopted by *McDonough and Sun* [1995], have been applied: (1) MgO ≤ 43 wt % and (2) [La/Yb]$_N$ ≤ 2. The first criterion eliminates the samples that are significantly depleted by melt extraction. Although *McDonough and Sun* [1995] rejected all samples with MgO concentrations higher than 40.5 wt % (thus retaining only most fertile peridotites), it was found out that adding relatively more depleted samples in the data set could better resolve compositional trends (Figure 1). The second criterion tries to exclude the peridotites that experienced metasomatic enrichment. The resulting data set contains 218 samples (103 xenoliths and 115 massif peridotites), which is not substantially different from that used by *McDonough and Sun* [1995]. We will treat massif peridotites and xenoliths collectively as mantle peridotites, as *McDonough and Sun* [1995] noted that these two types of peridotites are almost indistinguishable in terms of compositional trends.

[10] Note that we do not use any garnet peridotite in our analysis. Garnet peridotites are generally believed to have experienced more complex history, and it is probably unwise to include such samples. The global compilation by W. F. McDonough contains a large number of garnet
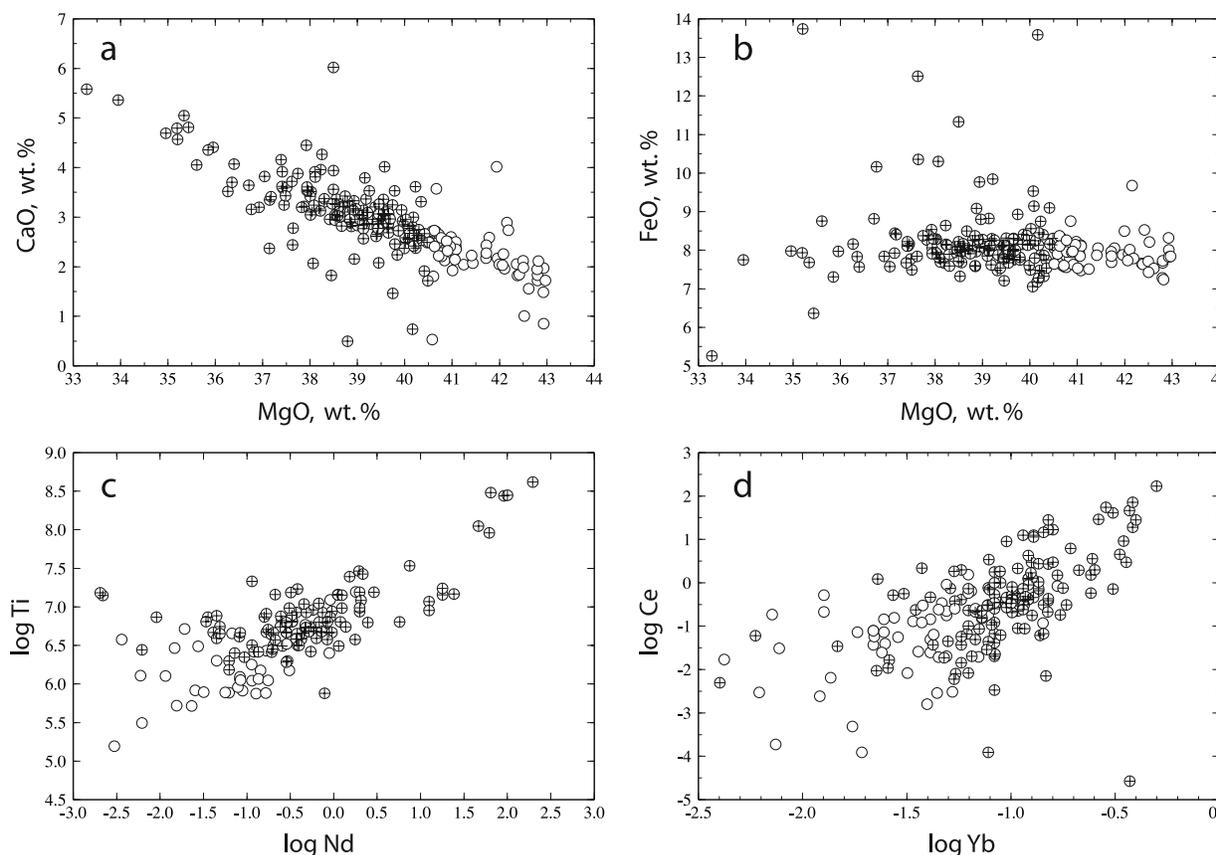
Figure 1. Some examples for covariation of chemical compositions in mantle peridotites used in this study. (a) CaO versus MgO, (b) FeO versus MgO, (c) Ti versus Nd, and (d) Ce versus Yb. Oxides are in wt %, and Ti, Nd, Ce, and Yb are in ppm. Crossed circles denote samples with MgO $\leq$ 40.5% (corresponding to the samples used by *McDonough and Sun* [1995]). Note that trace element covariations become nearly linear in the logarithmic space.

peridotites as well, but most of them do not pass the above two screening criteria anyway. In addition, because of our MgO criterion, the Mg # of the screened samples are mostly below 91. Thus our data do not include the so-called cratonic xenoliths from Archean terranes [*Boyd*, 1989; *Kelemen et al.*, 1998], and they lie on the "oceanic" trend as defined by *Boyd* [1989].

[11] One of the global features of mantle peridotites is that their Ca/Al ratio is, on average, ~15% higher than the chondritic value of ~1.1 [e.g, *Palme and Nickel*, 1985]. In the data set compiled for this study, the Ca/Al ratio varies from 0.5 to 3.6 with the mean value around 1.3 (Figure 2). The bulk Earth Ca/Al is expected to be chondritic, since both Ca and Al are RLEs, and the Ca/Al ratio is one of the most constant ratios among different chondritic groups. As a vast majority of mantle melts have Ca/Al ratio close to the chondritic value [e.g., *Manson*, 1967; *Melson et al.*, 1976], *Hart and Zindler* [1986] argued that the superchondritic Ca/Al ratios in relatively fertile peridotites are unlikely to be produced from simple melt extraction or enrichment of the primitive mantle material, and they suggested that the high Ca/Al in peridotites may be explained by local heterogeneity in mineral abundances. Modal heterogeneity on the scale of centimeters to meters is common in spinel lherzolites. It is thought to be caused by the segregation of the chromium-diopside suite of dikes in massif peridotites, which results in

more or less diffuse bands enriched or depleted in clinopyroxene (cpx) [*Palme and O'Neill*, 2003]. As Ca/Al is high in cpx, many peridotites enriched in cpx have superchondritic Ca/Al ratios. The cpx banding is also observed in mantle xenoliths [*Irving*, 1980], and the overall similarity of compo-
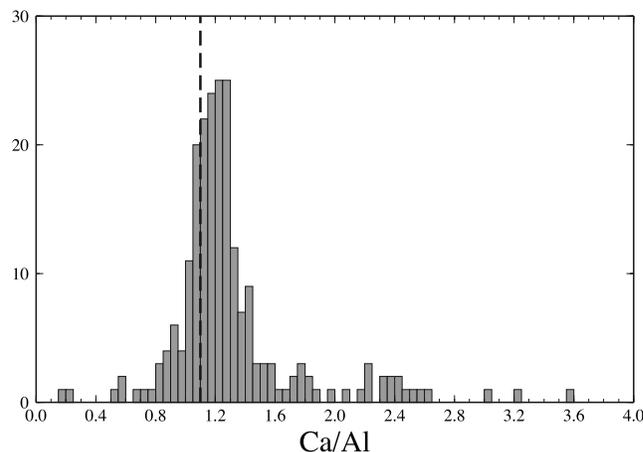
Figure 2. Histogram of Ca/Al ratio in peridotites (in the data set compiled for this study). The dashed line corresponds to the CI value of Ca/Al ~ 1.1.

sitional data of massif peridotites and xenoliths implies that this type of modal heterogeneity is ubiquitous in mantle peridotites.

[12] To mitigate the effect of the modal heterogeneity when constructing the PM model, *Hart and Zindler* [1986] proposed the so-called cpx correction, which forces the peridotite Ca/Al ratios to the chondritic value. *McDonough and Sun* [1995], however, argue that no correction is necessary to derive a PM model with the chondritic Ca/Al ratio. This issue is debatable, and the possibility of a nonchondritic Ca/Al ratio has important implications for the mantle structure [e.g., *Palme and Nickel*, 1985; *Walter and Trønnes*, 2004]. For this reason, we will use both raw data and cpx-corrected data when estimating the primitive mantle composition. The comparison of the two models and detailed discussion on cpx correction are given in section 5.2.

2.2. Meteorite Data

[13] We use the composition of CI chondrites to derive the bulk Earth ratios of refractory lithophile elements. There exist several different compilations of the CI chondrite composition, which vary by about 5–10% for most of the chemical elements [e.g., *McDonough and Sun*, 1995; *Lodders and Fegley*, 1998; *Palme and O'Neill*, 2003]. For this study we choose the model by *Lodders and Fegley* [1998], which is composed of selected values from six different compilations. We will use the CI ratios of RLEs as cosmochemical constraints when we implement a least squares minimization scheme. To account for the uncertainty of the CI composition, we will allow up to 5% deviations from our chosen CI model.

[14] The use of the CI chondrite data to constrain the RLE ratios in the bulk Earth is common in modeling Earth's composition [e.g., *Ringwood*, 1975; *Anderson*, 1989; *McDonough and Sun*, 1995]. This is because the CI-chondrite composition is usually regarded as a good representation of the mean nebular condensable material [*Wasson and Kallemeyn*, 1988; *Palme and Jones*, 2003]. Even though Earth is in many respects different from CI chondrites (i.e., depleted in nonrefractory elements, characterized by different oxygen isotopic composition, etc. [e.g., *Clayton and Mayeda*, 1996; *Drake and Righter*, 2002]), it is believed to retain the solar proportions of refractory lithophile elements. This assumption is strongly supported by terrestrial isotope data involving RLEs. The observed secular evolution of Nd and Hf isotopic ratios in igneous rocks is consistent with the bulk Earth Sm/Nd and Lu/Hf ratios being within ~5% of the chondritic ratios [e.g., *DePaolo and Wasserburg*, 1976; *Blichert-Toft and Albarède*, 1997]. There is no evidence for significant preaccretional fractionation of these four elements, Sm, Nd, Lu, and Hf, from the rest of RLEs. Moreover, the relative abundances of RLEs are approximately constant in all types of chondrites (carbonaceous, ordinary, and enstatite), even though there is a significant variation in the oxygen isotopic composition, oxidation state and volatile content. This suggests that refractory lithophile elements became fractionated only after they were accreted in a planet, and the primitive, undifferentiated Earth was likely to have nonfractionated relative abundances of these elements. The CI-chondrite RLE ratios is thus probably the most robust cosmochemical constraint on Earth's composition.

[15] A recent study on ^{142}Nd suggests that BSE Sm/Nd could be slightly nonchondritic [*Boyet and Carlson*, 2005], but the suggested deviation is still within the range of ±5% uncertainty used in our analysis. Their study indicates that if BSE^{147}Sm/^{144}Nd is actually 5–10% higher than the conventional reference (chondritic uniform reservoir or CHUR), 0.1966, this would satisfy both ^{142}Nd and ^{143}Nd data. This CHUR value corresponds to Sm/Nd of 0.3121, which is slightly lower than the CI value of 0.3260 (because CHUR is based on other carbonaceous chondrites). Thus, if the study of *Boyet and Carlson* [2005] is proved to be correct, it would imply that BSE Sm/Nd may be in the range of 0.328 to 0.343, which is almost entirely included in the ±5% uncertainty around the CI value (0.310–0.342). This issue is discussed in more detail in our companion paper.

[16] We also note that the use of the CI-chondrite composition to define the reference RLE ratios does not preclude the possibility of noncarbonaceous (i.e., ordinary and enstatite) chondrites as Earth's building blocks, because those chondrites also have similar RLE ratios.

3. Method
3.1. Problems With Previous Studies and Overview of the New Method

[17] As crust is the product of mantle melting, the chemical composition of Earth's mantle must be somehow reflected in the compositions of melt (usually basalts) as well as residue (peridotites). This complementary relationship between basaltic magmas and ultramafic peridotites provides a basis for estimating the primitive mantle composition. The first-generation PM models were constructed on the simple assumption that the composition of primitive mantle must lie somewhere between those of basalt and peridotite (see a review by *Ringwood* [1975]). This approach was further extended by *Anderson* [1983, 1989], who used four different components: mid-ocean ridge basalts, ultramafic rocks, continental crust, and kimberlite. These four components are combined such that the refractory lithophile elements in the bulk silicate Earth are in chondritic proportions. A major problem with this approach is that besides the nonuniqueness of the number and type of components involved, all of these building blocks have highly variable compositions, with trace elements concentrations varying by many orders of magnitude. It is thus unclear how to define the average compositions for the components involved in modeling, and how to take into account their compositional variability when quantifying the uncertainty of the PM model.

[18] On the other hand, some authors focused on the analysis of fresh and fertile ultramafic nodules, based on the assumption that some of these samples may have compositions very close or identical to that of PM [*Jagoutz et al.*, 1979; *Sun*, 1982; *Wänke*, 1981]. Although fertile mantle peridotites are usually very similar to each other in terms of major elements, they tend to be highly variable in terms of incompatible trace elements [*Jagoutz et al.*, 1979]. How to pick up the most "pristine" mantle sample is not clear, and it would be unwise to have the entire subsequent analysis rely on such a potentially subjective choice.

[19] Another attempt to determine the PM composition utilizes both geochemical and cosmochemical trends. The

method assumes that Earth belongs to a family of primitive objects sampled by chondritic meteorites. Earth's position in this family is determined by a crossing point of the chondritic trend and the fractionation trend for mantle peridotites [*Loubet et al.*, 1975; *Jagoutz et al.*, 1979; *Allègre et al.*, 1995, 2001]. A problem with this approach is that in most cases chondrites do not exhibit simple linear trends. A particular set of chondrite groups is usually chosen to be fitted by a line in a certain chemical space (e.g., ratio versus ratio plot), and other groups that do not lie on this trend are ignored. Different authors favored different chondritic groups (e.g., CI-ordinary-enstatite line by *Jagoutz et al.* [1979], or carbonaceous CI-CO-CM-CV line by *Allègre et al.* [1995, 2001]). Put another way, those cosmochemical "trends" are factitious; there is no obvious argument to justify choosing certain classes of chondrites while simply ignoring others.

[20] A more objective way to utilize cosmochemical data for defining the composition of the primitive mantle is to incorporate only certain features shared by all kinds of chondritic groups, such as the ratios of refractory lithophile elements. Most of these ratios are similar among different classes of chondrites [*Wasson and Kallemeyn*, 1988; *Lodders and Fegley*, 1998]. Therefore *Hart and Zindler* [1986] and *McDonough and Sun* [1995] used this type of chondritic constraints for locating the PM composition on terrestrial melting trends. Our method for constructing the PM model is also based on this concept, which combines terrestrial data and the most reliable cosmochemical data without making any assumptions about accretion and fractionation processes in the solar nebula. Since a melting trend, on which the primitive mantle composition is identified, is supported by a large number of mantle peridotite data, this approach is more stable compared to trying to find an intact primitive mantle sample (if any) in the field.

[21] While being probably most satisfactory among existing methods, this approach has several difficulties to be overcome when we actually implement it. In previous studies the melting trends of mantle peridotites have been approximated either by theoretical melting models [*Hart and Zindler*, 1986] or by linear regression [*McDonough and Sun*, 1995]. The theoretical modeling of mantle melting is nonunique, depending on melting modes and element partitioning. To avoid data analysis to be biased by such assumptions, an empirical approach seems more appropriate. However, using linear regression to quantify compositional trends assumes that melting produces a close-to-linear relationship between element abundances in peridotites. This may not be true in general. *Workman and Hart* [2005] show that as far as the composition of melting residue (i.e., peridotites) is concerned, modal fractional melting is a good approximation for more complicated melting models. For fractional melting the concentrations of two elements A and B in the residue, C_A and C_B, are related by the following power law:

$$C_B = \alpha C_A^{\beta}. \tag{1}$$

Here $\alpha = C_B^o/C_A^o$, where C_A^o and C_B^o denote the original concentrations prior to melting, and

$$\beta = \frac{(1-D_B)D_A}{(1-D_A)D_B}, \tag{2}$$

where D_A and D_B are solid-melt distribution coefficients for the two elements [e.g., *McBirney*, 1993]. It follows that a relation between two elements is close to linear only when their distribution coefficients are similar. Forcing linearity in compositional trends may thus yield erroneous results.

[22] Moreover, least squares regression is very sensitive to occasional outliers, and careful visual inspection is usually needed to eliminate them before regression. Linear regression is also biased more toward horizontal rather than vertical trends, because the cost function to be minimized is normally formulated with data misfit in the vertical coordinate. Thus the estimate of the PM composition can strongly depend on how we plot a particular chemical space, for example, with a RLE ratio on the vertical axis or on the horizontal axis (e.g., Figures 3a and 3b). Although the nonlinearity of melting trends can be avoided by using the logarithms of element concentrations, the bias of linear regression toward horizontal trends is still a problem even in the logarithmic space (Figures 3c and 3d).

[23] Another difficulty arises when different chondritic constraints result in different estimates for the PM composition (this happens rather frequently; see Figures 3d–3f). It is not simple to calculate the average of two or more different estimates and corresponding uncertainty, because those chondritic constraints tend to be correlated. Treating individual estimates as independent data would lead to unrealistically small uncertainty, when the number of RLE ratios involved becomes large.

[24] To handle these issues, we first model trends in the multidimensional compositional space through the principal component analysis (PCA). PCA is a standard multivariate technique, which transforms a set of correlated variables into a set of uncorrelated variables (called principal components) in order of decreasing significance [e.g., *Albarède*, 1996; *Gershenfeld*, 1998]. The first principal component thus represents the largest fraction of the original data that can be explained by a single parameter, and some (or all) of other components can usually be removed with a negligible loss of data variance. As we will demonstrate later, peridotite concentrations of many chemical elements can effectively be modeled by the first principal component only. This means that we can model the variation of peridotite compositions (in terms of selected elements) along the melting trend by a single controlling variable, q. This analytical parameterization of peridotite compositions greatly facilitates the subsequent analysis of the melting trend. The RLE ratios can be expressed as a function of q, and we define a cost function, χ^2, which summarizes all of chondritic constraints for RLE ratios. The primitive-mantle value of q (we call this q_{PM}) is then readily calculated by minimizing this cost function. The primitive mantle composition in terms of the elements used in PCA can be determined from this q_{PM}.

[25] As PCA itself cannot handle nonlinearity such as the power law relation (equation (1)), the data set is converted to the logarithmic space. Additional advantages of using the log scale include reducing the impact of outliers on data analysis and simplifying the treatment of concentration ratios (since division in the linear space transforms to subtraction in the log space).

[26] Large scatters exhibited by peridotite compositional data (Figure 1) are obviously a concern regarding the
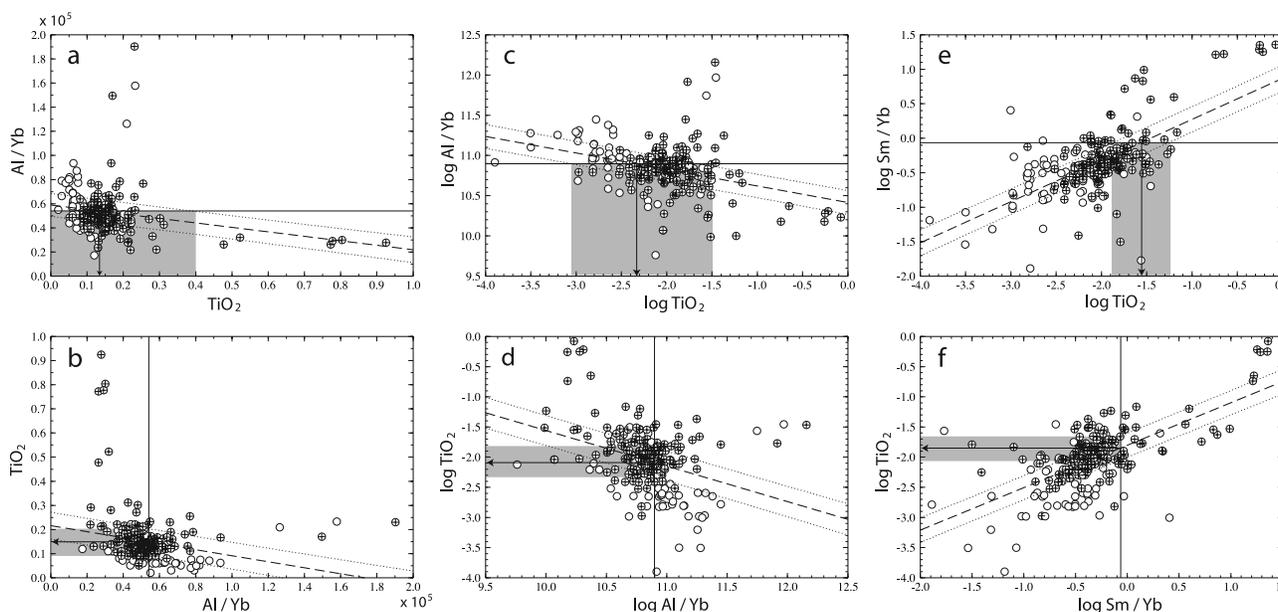
Figure 3. Examples of finding TiO_2 concentration in the primitive mantle using peridotite melting trends and chondritic RLE ratios. (Note that none of these approaches are used in our study. This is just to illustrate difficulties in modeling melting trends and imposing chondritic constraints.) Melting trend (shown as dashed) is modeled by linear regression; the uncertainty of the regression is shown as dotted lines. For chondritic constraints (solid lines), we use the CI composition by *Lodders and Fegley* [1998]. Crossed circles denote samples with $MgO \leq 40.5\%$ (corresponding to the samples used by *McDonough and Sun* [1995]). (a) Trend between TiO_2 and Al/Yb modeled in the linear space, with TiO_2 on the horizontal axis (this is the approach of *McDonough and Sun* [1995]). Gray shading indicates the range of PM concentration corresponding to chondritic Al/Yb. (b) Same as Figure 3a but with TiO_2 on the vertical axis. In terms of determining TiO_2 from chondritic constraints, this is preferred because TiO_2 should be modeled as a function of Al/Yb. Note that the range of estimated PM concentration is very different from Figure 3a. (c) Same as Figure 3a but in the log space. Trend is better resolved than in the linear space. (d) Same as Figure 3b but in the log space. (e) Same as Figure 3c but Sm/Yb instead of Al/Yb. (f) Same as Figure 3d but Sm/Yb instead of Al/Yb. Comparison of Figures 3d and 3f shows that different chondritic constraints can result in different estimates of PM concentrations.

quality of the melting trend defined by PCA. To measure the effect of those scatters and outliers on the above procedure and to translate them in terms of the uncertainty of the final PM model, we employ the bootstrap resampling method. This technique is based on producing a large number of quasi-independent ensembles from the original data by repetitive sampling. For each data ensemble, then, we apply the identical procedure: determine the controlling variable q by PCA, estimate q_{PM} by minimizing the cost function, and calculate the PM composition model from it. The statistics of resulting model ensembles is used to quantify the mean and variance of the PM composition. The bootstrap method may be regarded as conducting a large number of sensitivity tests with respect to scatters and outliers. It also allows us to propagate the uncertainty of all of model parameters involved in PCA and the cost function into the variance of the final PM model, by automatically taking into account parameter intercorrelation.

3.2. Single Controlling Variable and PCA

[27] Previous studies utilizing the trends of peridotite compositions all implicitly assume that the most significant trend is produced by variation in the degree of melting. This assumption may require justification, since the concentra-

tions of elements in melt and residue are determined not only by the degree of melting but also by *how* mantle melts. For example, hotter-than-normal mantle, when it ascends adiabatically, crosses the mantle solidus and starts to melt at a greater pressure. Therefore, for a given degree of melting hotter mantle melts under higher pressure and temperature conditions than "normal" mantle. Element partitioning between solid and liquid is often very sensitive to a change in pressure and/or temperature. Consequently, major compositional trends, in general, may be due not to different degrees of melting, but to the variation of other variables such as different pressures. Nonetheless, we can make at least two important observations for the peridotite data set used in this study, which suggest that its major compositional trends are mainly controlled by the degree of melting.

[28] First of all, mantle peridotites in general, and those from our data set in particular (Figure 1b), are characterized by a very limited variation in the iron content [e.g., *Palme and O'Neill*, 2003]. For most of the samples used in this study, their FeO contents are confined to the narrow interval of 8.01 ± 0.58 wt %, with the exception of a few outliers. On the other hand, it is well established that the Fe concentration of melt (and therefore that of residual mantle as well) is a strong function of pressure [e.g., *Klein and*

Table 1. Subsets for Constructing the PM Model[a]

	Subset	n[b]	Raw Data Set			The cpx-Corrected Data Set		
			$\lambda_1/\Sigma\lambda_i$[c]	EF $\pm \sigma$[d]	Mg $\pm \sigma$,[e] wt %	$\lambda_1/\Sigma\lambda_i$[c]	EF $\pm \sigma$[d]	Mg $\pm \sigma$,[e] wt %
1	**Nd Sm Eu Yb Ti Al Ca** Mg Si Fe	147	84.3	2.06 ± 0.37	23.5 ± 0.9	82.1	1.99 ± 0.39	24.0 ± 1.0
2	**La Ce Sm Yb Tb Al Ca** Mg Si Fe	164	83.5	2.24 ± 0.43	23.3 ± 0.9	82.4	2.03 ± 0.42	23.8 ± 1.0
3	**La Ce Nd Sm Yb Al Ca** Mg Si Fe Ni	117	83.9	2.10 ± 0.34	23.3 ± 1.1	83.4	1.98 ± 0.37	23.6 ± 1.0
4	**Nd Sm Eu Yb Lu Al Ca** Mg Mn Cr	120	82.5	2.17 ± 0.36	23.5 ± 0.9	76.7	1.96 ± 0.42	23.9 ± 1.0
5	**Sm Eu Yb Ti Al Ca Sc** Mg Zn V	86	86.7	2.18 ± 0.25	23.5 ± 0.8	81.9	2.03 ± 0.25	23.9 ± 0.9
6	**La Ce Sm Yb Al Ca** Mg Co Na	113	80.3	2.24 ± 0.43	23.3 ± 0.9	74.7	2.04 ± 0.43	23.7 ± 1.0
7	**Ti Al Ca** Mg	218	68.4	2.08 ± 0.67	23.6 ± 1.0	68.2	2.00 ± 0.78	23.9 ± 1.1
8	**Yb Al Ca Sc** Mg	185	72.1	2.25 ± 0.57	23.5 ± 1.0	77.5	2.15 ± 0.59	23.8 ± 1.0

[a]The subsets of chemical elements used for constructing the PM model (subsets 1 through 6) and for testing the stability of this model (subsets 7 and 8), with the results based on 10,000 accepted bootstrap solutions. Boldface indicates the refractory lithophile elements.

[b]A number of samples in a subset. The subsets are composed of the peridotite samples that contain measurements for all the chemical elements in the subset. Note that this condition reduces the size of subset 5 because of comparatively scarce database for V.

[c]Amount of the data variance explained by the first principal component; λ_i is the i eigenvalue of the data set covariance matrix, λ_1 is the largest eigenvalue. For the raw data set, $\lambda_1/\Sigma \lambda_i >80\%$ in all of main subsets (1–6). In the cpx-corrected data set, however, $\lambda_1/\Sigma\lambda_i$ slightly decreases.

[d]The median and the one standard deviation for the RLE enrichment factor.

[e]The median and the one standard deviation for Mg abundance in the primitive mantle.

Langmuir, 1987; *Kinzler and Grove*, 1992; *Walter*, 1998]. The approximately constant Fe content in our peridotite data set, therefore, indicates that these rocks have experienced melting under similar pressure conditions.

[29] Moreover, since the MgO concentration in the data set is limited to that below 43 wt %, the corresponding Mg # mostly falls in the range of 88.5–91.0. Mg # is a good measure of the degree of melting (with higher Mg # for more depleted residue), and the high end of this range roughly corresponds to ~20% of melting [*Langmuir et al.*, 1992; *Kinzler and Grove*, 1992]. As melting proceeds, mantle temperature decreases due to adiabatic decompression and the latent heat of fusion, so this limited degree of melting indicates that our samples have experienced melting within a rather restricted temperature range as well. Therefore it seems reasonable to assume that the major compositional trend in our peridotites is indeed produced by different degrees of melting.

[30] Note that we are not assuming single-stage melting. Given the presence of large scatters, the observed compositional trends may be better regarded as the sum of multiple events of melting and refertilization, and in this case, the "degree of melting" has only an approximate meaning. An important point is that as demonstrated later, these trends do pass through the "primitive mantle" point, which satisfies all of chondritic constraints. The exact origin of the compositional trends is thus not important for our analysis.

[31] When the concentrations of many elements appear to correlate with each other and they form a major compositional trend (here identified as the melting trend), we should be able to model those concentrations in terms of a single parameter (i.e., the degree of melting). Mathematically, this is equivalent to conducting PCA for given compositional data and taking the first principal component as a single parameter. PCA is frequently used to reduce the dimensionality of a given data set and discover its most concise representation. Here we are considering the extreme case of one-dimensional representation for the peridotite compositional space. Of course, not the entire compositional space can be adequately treated with a single parameter, so a part of the compositional space (hereinafter referred to as a "subset") is first identified to maximize the efficiency of PCA. Most of the elements in a subset must have correlated

concentrations. This ensures that the first principal component explains most of the variance of the subset. Moreover, a subset must include more than a few refractory lithophile elements. As we use only chondritic RLE ratios as cosmochemical constraints, the number of refractory lithophile elements is directly related to the number of chondritic constraints; a larger number of constraints should lead to a more stable model for PM composition. The choice of a subset is not unique, and for this study we construct several subsets with different refractory and nonrefractory elements (Table 1).

[32] Figure 4 shows the PCA results for one of the subsets used in this study. Element concentrations are expressed in terms of the first principal component (q), which reflects the degree of melting in peridotites. Therefore the concentrations of highly incompatible elements vary significantly with q (i.e., characterized by steep slopes), whereas those of slightly incompatible or compatible elements are approximately constant for different q.

[33] Being a standard multivariate method, the description of PCA can easily be located elsewhere [e.g., *Albarède*, 1996; *Gershenfeld*, 1998]. Our extended usage of PCA with a particular emphasis on the first principal component is, however, not common, and thus it requires some explanation. The details of mathematical derivation are given in Appendix A, and we just summarize the main points below.

[34] We denote a data set composed of n samples with the concentrations of m elements by $\{C_i^j\}$, with the subscript i as the element index and the superscript j as the sample index, i.e., $i = 1, 2,.., m$, and $j = 1, 2,.., n$. A corresponding lognormalized data set, $\{p_i^j\}$, may be constructed by

$$p_i^j = \log C_i^j - \mathcal{E}(\log C_i), \tag{3}$$

where $\mathcal{E}(\log C_i)$ denotes the mean of $\log C_i$, i.e.,

$$\mathcal{E}(\log C_i) = \frac{1}{n}\sum_j \log C_i^j. \tag{4}$$

Note that this lognormalized data set has zero mean:

$$\mathcal{E}(p_i) = 0. \tag{5}$$
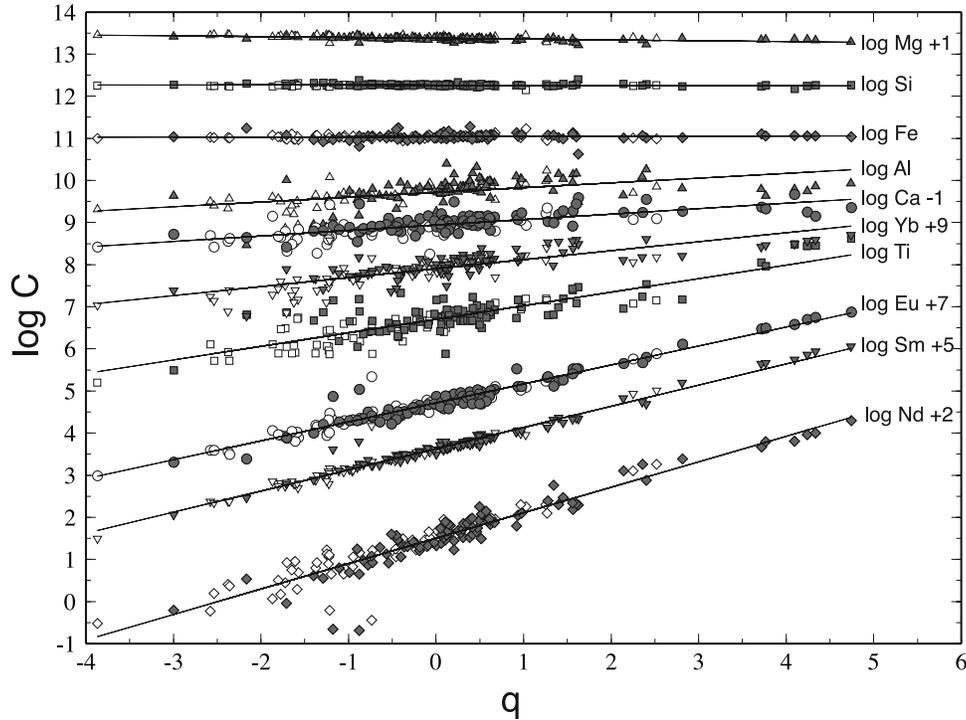
Figure 4. Modeling the peridotite melting trends with PCA for subset 1 (Table 1). Log concentrations (in ppm) of all the elements in the subset are represented as a function of q, which corresponds to the degree of melting. Shaded symbols denote samples with $MgO \leq 40.5\%$ (corresponding to the samples used by *McDonough and Sun* [1995]). Log concentrations of some elements (Mg, Ca, Yb, Eu, Sm, Nd) in a plot are shifted in vertical direction (indicated by +1, etc.) for the sake of clarity.

As described in Appendix A, PCA is essentially solving an eigenvalue problem for the covariance matrix of this data set. When this data set can effectively be modeled by the first principal component only, the single controlling variable q can be calculated (for each data j) as

$$q^j = a_1 p_1^j + a_2 p_2^j + \cdots + a_m p_m^j, \tag{6}$$

where $[a_1 \; a_2 \cdots a_m]$ is the eigenvector corresponding to the largest eigenvalue. It can also be shown that the part of the original data explained by the first principal component can be expressed as

$$\widetilde{p}_i^j = q^j a_i. \tag{7}$$

Recalling the definition for the lognormalized data set (equation (3)), we see that the part of compositional data perfectly correlating with the most dominant trend (e.g., melting trend) can be expressed as

$$\log \widetilde{C}_i^j = q^j a_i + \mathscr{E}(\log C_i). \tag{8}$$

[35] While the correlated part of peridotite data is described by the first principal component, the uncorrelated part, which corresponds to random scatters around the melting trend, is distributed among all the other components. Those minor components usually contain less than 20% of the data variance (Table 1). To account for this residual variance when modeling the peridotite data, we

introduce a random variable ω, which follows a Gaussian distribution with zero mean and variance σ. A random variable is a mathematical notation to describe the outcome of a random process, and here it is used to model the influence of various unspecified processes on the melting trend. For each chemical element i, σ_i denotes the standard deviation of actual peridotite composition from predicted composition (equation (8)):

$$\sigma_i = \sqrt{\frac{1}{n} \sum_{j=1}^{n} \left(\log C_i^j - \log \widetilde{C}_i^{\,j} \right)^2} \; . \tag{9}$$

[36] The peridotite compositional data can thus be regarded as a sum of the correlated part, corresponding to melting processes in the mantle (equation (8)), and random noise ω_i:

$$\log C_i(q) \approx q a_i + \mathscr{E}(\log C_i) + \omega_i. \tag{10}$$

The controlling variable q can be used to reproduce the concentration of any element in the subset along the melting trend (Figure 4). Once the value of q corresponding to the primitive mantle is estimated, the PM concentrations of all elements in the subset can be easily found.

[37] The explicit modeling of the noise component in peridotite data with the stochastic parameter ω (equation (10)) is an important part of our method, since it allows us to take into account the compositional variability of mantle
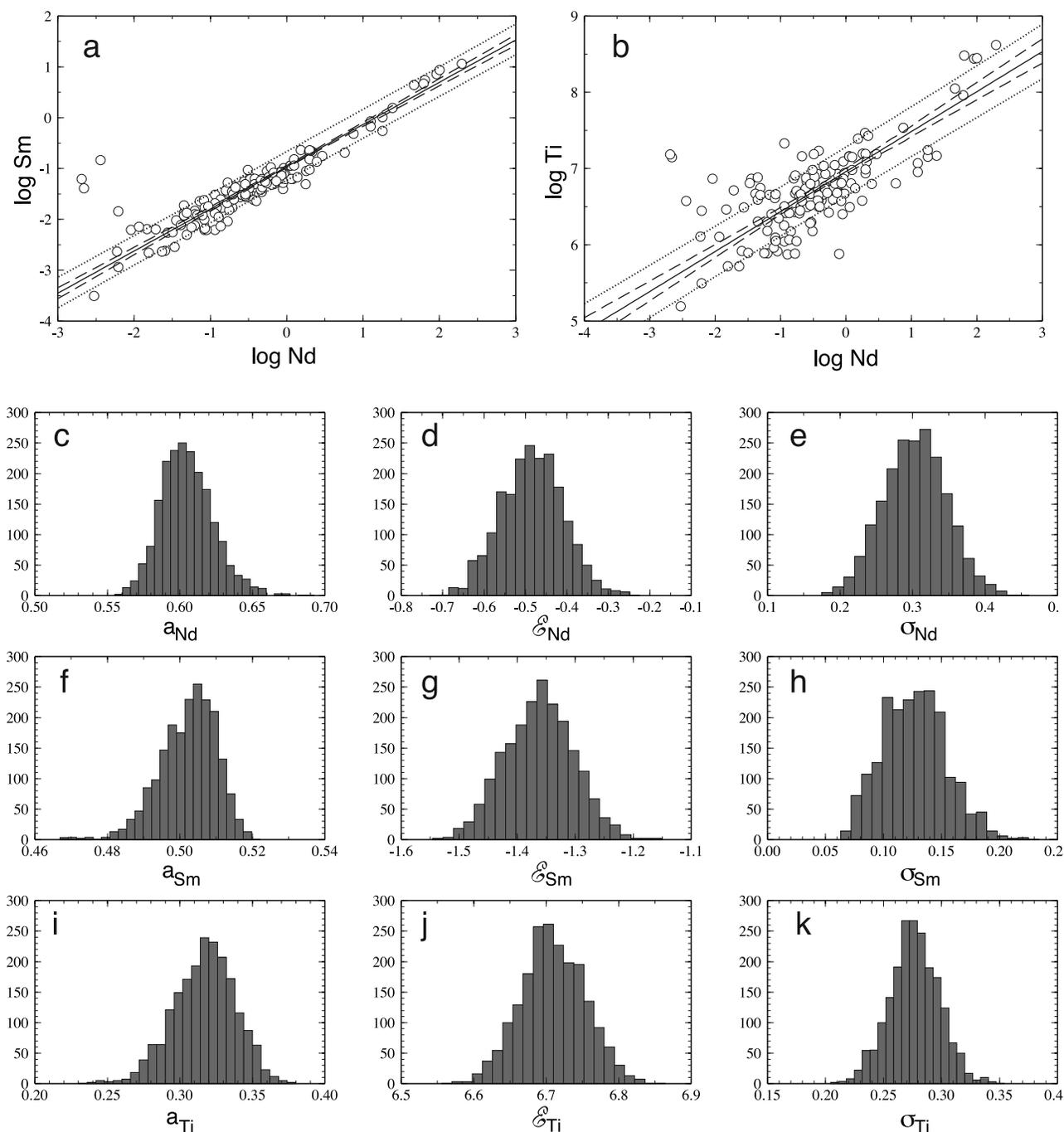
Figure 5. Modeling melting trends with PCA and bootstrap resampling technique: (a) logNd versus logSm space and (b) logNd versus logTi space. Solid lines represent the mean trend for 2,000 bootstrap ensembles. Dashed lines are one standard deviation from those trends for a case when only the correlated part of the data is taken into account. Dotted lines correspond to one standard deviation from the mean, when the scatters in peridotite data are modeled with the stochastic component. (c–k) Bootstrap distributions of the PCA coefficients, mean values in peridotite data set and σ_i for log Nd (Figures 5c–5e), log Sm (Figures 5f–5h), and log Ti (Figures 5i–5k).

peridotites when constructing the PM model. Using only the correlated part of compositional data (equation (8)) is not sufficient for adequate modeling of melting trends, even when we use the bootstrap resampling technique to account for the effects of data scatters and outliers (section 3.4). Figures 5a and 5b shows an example of modeling the

peridotite melting trends with and without the noise component. Obviously, when the noise component is taken into account, the uncertainty range of the melting trend is much larger compared to that derived from the correlated part of the data alone. This large uncertainty is consistent with the actual compositional variations in peridotite data. Incorpo-

rating the noise component thus provides us a realistically wide compositional space, which is important when we locate the primitive mantle composition with multiple chondritic constraints. The implementation details of the stochastic procedure for modeling the noise component are given in section 3.3.

3.3. Chondritic Constraints and Cost Function

[38] The value of q corresponding to the primitive mantle (q_{PM}) can be derived using the cosmochemical constraints, i.e., chondritic values for RLE ratios. By varying q, one goes up or down the melting trend, and concentration ratios change accordingly. There should exist (at least) one point on the melting trend, where the corresponding concentration ratios are *least conflicting* with the chondritic constraints. This is equivalent to finding the optimal q by minimizing a cost function, which quantifies deviation from all of imposed constraints.

[39] We formulate our cost function based on the RLE enrichment factor. This enrichment factor is defined as the concentration of the refractory lithophile elements in Earth, normalized to their CI concentration. We denote the logarithmic enrichment factor for element i, which belongs to RLEs, as

$$\varepsilon_i = \log C_i(q) - (\log C_i)_{\text{CI}}, \tag{11}$$

where $(\log C_i)_{\text{CI}}$ is log concentration of element i in the CI chondrites.

[40] Since Earth is assumed to possess the RLEs almost exactly in CI proportions, the enrichment factors ε_i corresponding to different RLEs should coincide. The cost function χ^2 thus quantifies deviations of the individual enrichment factors from their mean value:

$$\chi^2(q) = \sum_i (\varepsilon_i - \bar{\varepsilon})^2, \tag{12}$$

where $\bar{\varepsilon}$ denotes the mean enrichment factor:

$$\bar{\varepsilon} = \frac{1}{N} \sum_i \varepsilon_i.$$

[41] Our cost function is quadratic in q and also nonnegative, so it has only one minimum, which uniquely defines q_{PM}. The minimization of the cost function is done by solving $d\chi^2(q)/dq = 0$, which leads to

$$q_{PM} = -\frac{\sum_i b_i d_i}{\sum b_i^2}, \tag{13}$$

where

$$b_i = a_i - \frac{1}{N} \sum_i a_i,$$

$$d_i = \mathcal{E}(\log C_i) - (\log C_i)_{\text{CI}} + \omega_i$$
$$- \frac{1}{N} \sum_i \left(\mathcal{E}(\log C_i) - (\log C_i)_{\text{CI}} + \omega_i \right).$$

[42] We model the random noise component in equation (13) with Monte Carlo simulations, by drawing random numbers from Gaussian distribution with standard deviation of σ_i (equation (9)). This provides us with a number of different noise representations and, consequently, with a number of slightly different q_{PM} (equation (13)). Each of those q_{PM} can be used to find a corresponding primitive mantle concentration for all of the elements involved in modeling (equation (10)). However, these different PM models are not of equal quality. Some noise representations result in larger χ^2 than others; larger χ^2 corresponds to less consistent enrichment factors (equation (12)). As we allow only up to 5% deviation from our CI model, we must reject PM models with larger deviations (Figure 6). The rejection rate turns out to be rather high, given the small tolerance for deviation, and noise simulation has to be iterated (with some maximum number of iteration) until an acceptable PM model is found. As noted earlier, the use of the noise component is essential. Without it, the compositional space for peridotite melting is too limited, and finding a chondritic PM composition becomes difficult (Figures 5a and 5b).

3.4. Bootstrap Resampling

[43] Although the above procedure for deriving the q_{PM} tries to take into account the uncertainty of the melting trend by stochastic inversion, it does not fully capture the effects of data scatters because the random component in equation (10) fluctuates only around the uniquely defined melting trend for a given subset. That is, we are assuming that the PCA coefficients $\{a_i\}$ and the log mean of concentration $\{\mathcal{E}(\log C_i)\}$ have no errors, but such an assumption is unlikely to be valid. We may cast the uncertainty issue as the sensitivity of these PCA parameters to perturbations to a given data set. If we randomly drop a few samples, for example, how these parameters would change? In the absence of scatters, they would stay the same. If we have scattered data, on the other hand, they may vary substantially, indicating that isolating the first principal component (and deriving the PM composition) is subject to large uncertainty.

[44] The bootstrap resampling method is probably best suited to quantify this type of uncertainty. This sampling theory approach to statistical inference is based on the idea that real data arise as one ensemble (or realization) from some conceptual probability distribution, $\mathcal{F}$. The uncertainty of our inference can be measured if we can estimate $\mathcal{F}$. In most cases, however, the conceptual distribution $\mathcal{F}$ is unknown. The bootstrap method approximates this distribution by the sampling distribution $\mathcal{F}_s$ based on original data. In practice, this means that if our original data are composed of n samples, $\{x_j\} = x_1, x_2, \ldots x_n$, we can create another ensemble by randomly drawing a sample n times from this $\{x_j\}$ with repetitive sampling allowed (note: if repetitive sampling is not allowed, and if we draw only $(n - 1)$ times, we have the jackknife method instead). This ensemble is called a bootstrap ensemble. By repeating this random resampling, we can create a number of bootstrap ensembles or pseudodata sets. This may sound circular (and the name "bootstrap" also implies so) because those bootstrap ensembles are statistically independent to each other only under the assumption of $\mathcal{F}_s \approx \mathcal{F}$. One can, however, also regard this procedure as conducting a large number of sensitivity tests. For each of bootstrap ensembles, we conduct PCA, estimate q_{PM}, and derive the PM composition
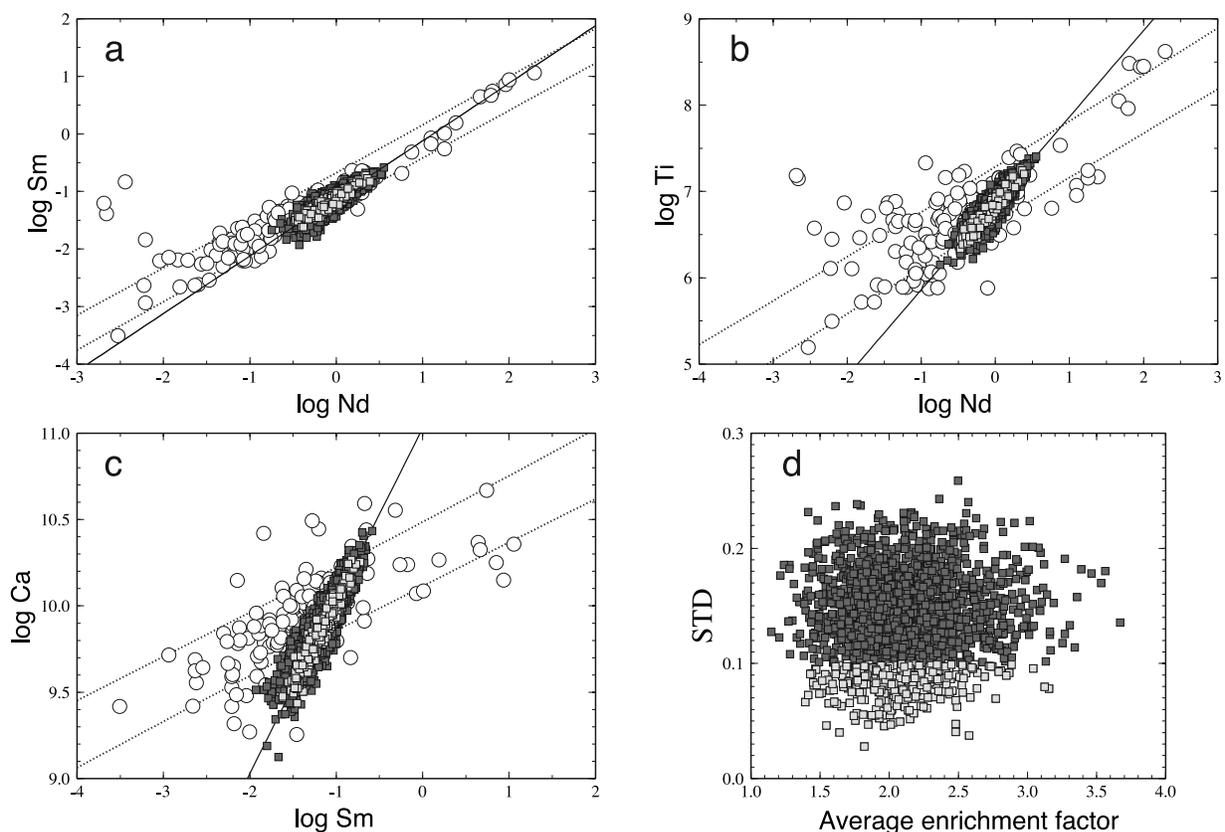
Figure 6. Example of using the Monte Carlo simulations for modeling the noise component in peridotite date when deriving the PM composition. Uncertainty range for melting trends in (a) log Nd versus log Sm, (b) log Nd versus log Ti, and (c) log Sm versus log Ca shown with dotted lines. Solid lines denote the chondritic constraint. Squares correspond to all the PM models derived from ~2000 bootstrap ensembles. Light shaded squares correspond to the accepted models, with RLE enrichment factors deviating within 5% from their mean (assuming mean value at 2.0). (d) Distribution of the average RLE enrichment factor for all the bootstrap ensembles (open squares) and the accepted solutions (shaded squares) versus the standard deviation of individual enrichment factors from the average.

(see Figures 5c–5k for the bootstrap distributions of some PCA parameters). From M bootstrap ensembles, therefore, we have M different estimates of the PM composition, and the final PM composition and its uncertainty can be derived from the statistics of these M estimates.

[45] Thus the bootstrap method allows us to directly map scatters in the original data into the variance of the final composition model. As our procedure of estimating the PM composition is not a single step (i.e., we first determine the melting trend and then impose chondritic constraints), it would be highly cumbersome to use standard error propagation rules to map data variance into model uncertainty, by correctly taking into account correlation among parameters (which involves error covariance matrix). Standard propagation rules also assume the Gaussian distribution of errors, which may not always be valid. The bootstrap method is a simple but brute force alternative, and it is a tractable option in our case because calculating q_{PM} for one ensemble is computationally inexpensive.

4. Results

[46] We use the above scheme to directly compute the PM abundances of 22 chemical elements. As we cannot con-

struct a satisfactory one-dimensional representation for all those elements simultaneously, we build several subsets, each of them containing not more than eleven elements. The subsets are compiled such that most of the elements have correlated concentrations; this ensures that the amount of data variance explained by the first principal component is sufficiently high (i.e., greater than ~80%). Each of the subsets contains six or seven RLEs (providing up to 24 different chondritic ratios for defining the PM composition), and a small number of nonrefractory elements. Each of them also includes Mg; this helps us to test if different subsets yield similar PM abundance of Mg, regardless what elements and chondritic constraints are used in their construction. The six different subsets that we construct for this study cover 12 refractory and 10 nonrefractory elements (Table 1). Additionally, for the sake of discussion, we will also present the results for a subset that includes only major and minor elements, and another one composed of only moderately and slightly incompatible elements (those results will not be taken into account when constructing our final PM model). These subsets (subsets 7 and 8, Table 1) are designed to see how the use of trace RLEs and highly incompatible RLEs in reconstructing the peridotite melting trends affects the resultant PM model.
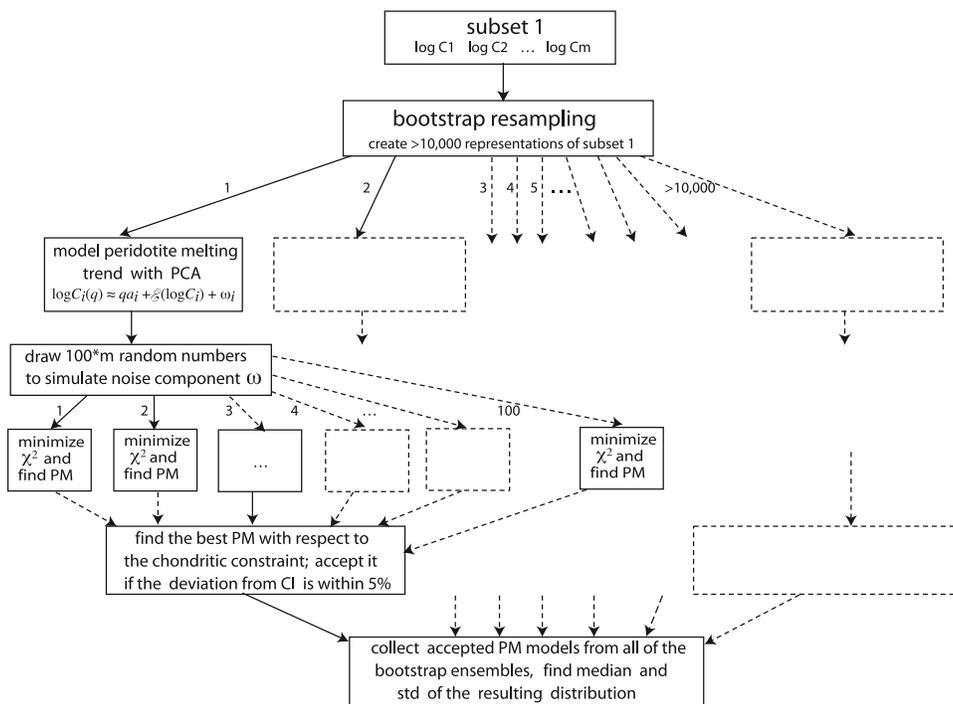
Figure 7. Block diagram of our method for deriving the PM composition. For each of the six subsets used in constructing our PM model we first create a large number of different bootstrap ensembles (more than 10,000). For each of the bootstrap ensembles we perform the PCA to extract the part of the data that corresponds to the first principal component (i.e., the melting trend). The residual part of the data variance (i.e., random scatters in peridotite compositions) is modeled with 100 Monte Carlo simulations. On the next step we compute the q_{PM} value and the corresponding PM composition with each of the noise simulations, thus obtaining a set of 100 slightly different PM models for each of the bootstrap ensembles. The acceptable PM composition (with regard to the chondritic constraint) should have individual enrichment factors deviating from their mean by less than 5%. If none of the $\sim 10^2$ different PM compositions in a bootstrap ensemble is within the 5% of the chondritic constraint, this bootstrap ensemble is rejected. If there are more than one satisfactory PM compositions, we choose the one with the smallest χ^2. Finally, we collect the acceptable PM models from all of the bootstrap ensembles. Taking the statistics of all those acceptable PM models gives us the median and the standard deviation of the PM concentrations for all the elements in a subset.

[47] With the subsets compiled, the implementation of our three-step procedure for deriving the PM composition is the following (see Figure 7 for the block diagram of our method). In each subset we first create a large number of different bootstrap ensembles by resampling from the original data set. For each of the bootstrap ensembles we perform the PCA to extract the part of the data that corresponds to the first principal component (i.e., the melting trend). The residual part of the data variance (i.e., random scatters in peridotite compositions) is modeled with $\sim 10^2$ Monte Carlo simulations. Note that the number of noise simulations does not influence the result of the modeling, and only affects the rate of finding the acceptable PM solutions. On the second step we compute the q_{PM} value and the corresponding PM composition with each of the noise simulations, thus obtaining a set of $\sim 10^2$ slightly different PM models for each of the bootstrap ensembles. The acceptable PM composition (with regard to the chondritic constraint) should have individual enrichment factors deviating from their mean by less than 5%. If none of the $\sim 10^2$ different PM compositions in a bootstrap ensemble is within the 5% of the chondritic constraint, this bootstrap ensemble is rejected. If there are more than one satisfactory PM compositions, we choose the one with the smallest χ^2. Finally, we collect the acceptable PM models from all of the bootstrap ensembles. The bootstrap resampling is continued until we obtain a statistically significant distribution of the PM compositions. In this study, we gathered 10^4 acceptable PM models for each of the six subsets; this required constructing from $\sim 2 \times 10^4$ to $\sim 6 \times 10^5$ individual bootstrap ensembles. Taking the statistics of all those acceptable PM models gives us the median and the standard deviation of the PM concentrations for all the elements in a subset (we use median rather than mean values, since the bootstrap distributions may be slightly asymmetric, Figure 8a). The results of those calculations for the raw peridotite data as well as the cpx-corrected data are presented in Table 1. Although our method does not explicitly impose the closure property for the PM composition, the sum of major oxides is 99.0 ± 0.5 wt % before normalization.
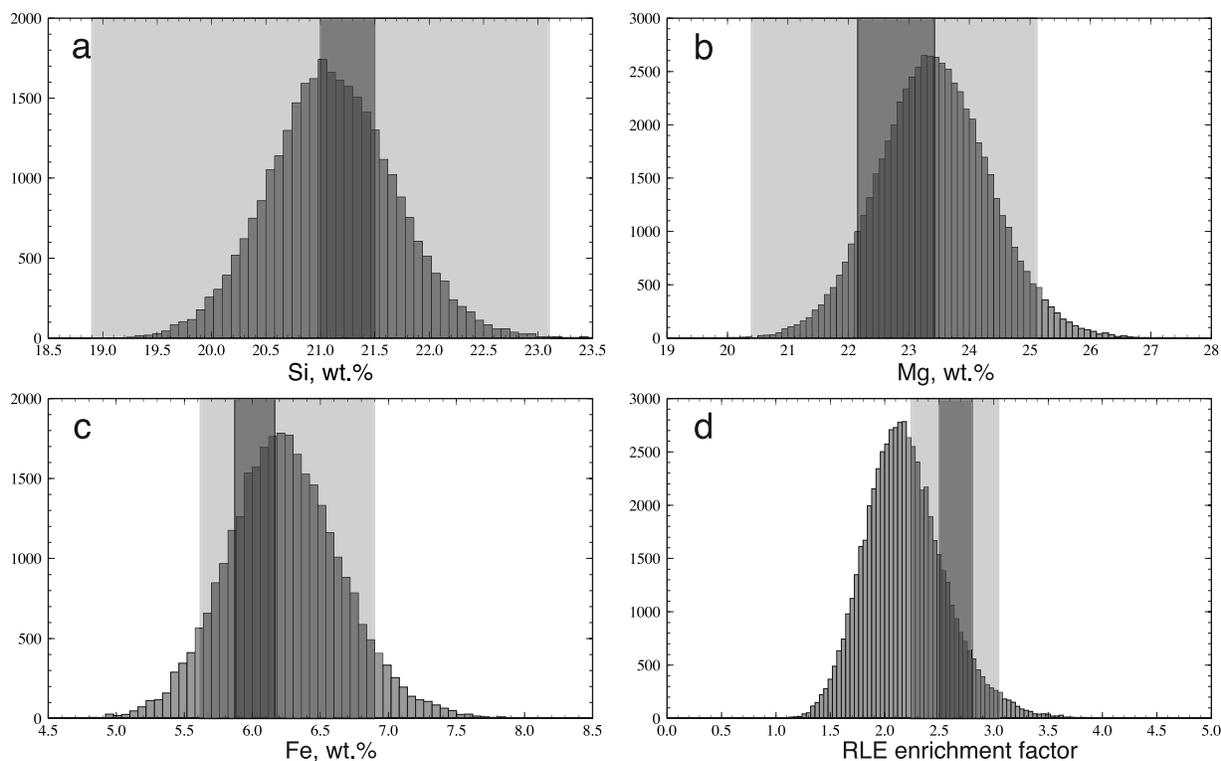
Figure 8. Bootstrap distributions of the primitive mantle abundance of (a) Si, (b) Mg, (c) Fe, and (d) the RLE enrichment factor, based on the integrated results from subsets 1–6. Dark gray shading corresponds to the mean values of the previous estimates of these parameters [*Hart and Zindler*, 1986; *McDonough and Sun*, 1995; *Palme and O'Neill*, 2003]. Light gray shading corresponds to uncertainty intervals in those models.

[48] All of the six subsets yield similar estimates of the RLE enrichment factor and Mg abundance in the primitive mantle, despite different sets of constraints that were used to locate the PM composition. The use of light REE in these subsets may disconcert many geochemists, because the concentrations of such highly incompatible elements in mantle peridotites could easily be modified by metasomatic events [e.g., *Jochum et al.*, 1989]. We can, however, still identify covariation between those highly incompatible elements and less incompatible elements (e.g., Ce versus Yb in Figure 1d), though such trends usually have large scatters. There are both an advantage and a disadvantage in using highly incompatible elements. On one hand, they could potentially better constrain the PM composition because their trends have steeper slopes (e.g., Figure 4). On the other hand, they have larger scatters, which make our estimate more uncertain. Our results summarized in Table 1 indicate that the above advantage appears to more than compensate the disadvantage, because the results for the subsets without light REE (7 and 8) are very similar to those with light REE (1 through 6), except that the latter have smaller uncertainty for the enrichment factor. That is, the use of light REE does not introduce any bias and only helps to sharpen our statistical inference. We also remind readers that our data selection (section 2.1) already excluded at the outset many samples that are likely to have experienced secondary enrichment processes. Our results also show that certain volatile and siderophile elements (e.g.,

Ni, Na, Co, V) has no negative effects on our resultant PM model.

[49] The effect of the cpx correction on the estimated PM composition is not significant: for the raw data the RLE enrichment factor in different subsets varies from 2.05 to 2.25, whereas for the cpx-corrected data it varies from 1.95 to 2.15. This difference is barely notable, since the average uncertainty of our estimate of the enrichment factor is ∼0.3. Similarly, the estimates of the primitive mantle Mg abundance are only slightly higher in the cpx-corrected data set compared to the raw data, and this difference is within uncertainty. Therefore we will adopt the PM model based on the raw data set hereinafter; further discussion on the cpx correction and the possibility of the nonchondritic Ca/Al ratio in the upper mantle will be given in section 5.2.

[50] Having confirmed that all of the six subsets result in practically the same primitive mantle composition, we derive an integrated PM model by combining the accepted solutions for all subsets. The integrated estimates are thus based on ∼6×10^4 solutions for the RLE enrichment factor and Mg, and on ∼3×10^4 solutions for Fe and Si (Figure 8).

[51] Our final PM model is very close to the previous models in terms of Mg, Si and Fe (Table 2). Our estimate of the Mg concentration in the PM is 23.41 ± 0.93 wt %, the median being only slightly higher than the preferred values in the previous models (22.2 ∼ 22.8 wt %), and the one standard deviation interval overlapping the reported uncertainty intervals in those models. The estimates of Si and Fe

Table 2. Models of the Primitive Mantle Composition[a]

	Hart and Zindler [1986]	McDonough and Sun [1995]	Palme and O'Neill [2003]	This Study
Mg, %	22.8 ± 0.6	22.8 ± 2.3	22.17 ± 0.22	23.41 ± 0.93
Si, %	21.5 ± 0.6	21.0 ± 2.1	21.22 ± 0.21	21.09 ± 0.58
Fe, %	∼5.86[b]	6.26 ± 0.63	6.30 ± 0.06	6.22 ± 0.42
RLE enrichment factor	2.51 ± 0.25	2.75 ± 0.23	2.80 ± 0.23	2.16 ± 0.37
K, ppm	∼266[b]	240 ± 48	260 ± 39	190 ± 40
U, ppb	20.8	20.3 ± 4.1	21.8 ± 3.3	17.3 ± 3.0
Th, ppb	–	79.5 ± 11.9	83.4 ± 12.5	62.6 ± 10.7
SiO_2, %	45.96 ± 1.33	44.9 ± 4.5	45.5 ± 0.46	44.95 ± 1.24
TiO_2, %	∼0.181[b]	0.201 ± 0.020	0.214 ± 0.021	0.158 ± 0.027
Al_2O_3, %	4.06 ± 0.04	4.43 ± 0.44	4.51 ± 0.36	3.52 ± 0.60
Cr_2O_3, %	∼0.468[b]	0.383 ± 0.058	0.369 ± 0.074	0.385 ± 0.057
MnO, %	∼0.130[b]	0.135 ± 0.014	0.136 ± 0.013	0.131 ± 0.012
FeO, %	∼7.54[b]	8.04 ± 0.80	8.12 ± 0.08	7.97 ± 0.54
NiO, %	∼0.277[b]	0.249 ± 0.025	0.237 ± 0.012	0.252 ± 0.027
MgO, %	37.8 ± 1.0	37.8 ± 3.8	36.85 ± 0.37	39.50 ± 1.53
CaO, %	3.21 ± 0.03	3.53 ± 0.35	3.66 ± 0.037	2.79 ± 0.47
Na_2O, %	∼0.332[b]	0.359 ± 0.054	0.350 ± 0.018	0.298 ± 0.141
K_2O, %	∼0.032[b]	0.029 ± 0.06	0.031 ± 0.005	0.023 ± 0.005
P_2O_5, %	∼0.019[b]	0.021 ± 0.003	0.020 ± 0.015	0.015 ± 0.003
Mg#	89.9 ± 0.2	89.3 ± 2.1[c]	89.0 ± 0.1[d]	89.6 ± 1.0

[a]Oxide concentrations are normalized to 100%.

[b]The PM concentrations of these elements are derived through mass balance calculation accounting for Earth's core from the CI model of Earth's composition (assuming that Earth represents the end-member of enstatite-ordinary-CI-CM2 trend in meteorite data).

[c]This uncertainty is based on 10% uncertainty reported for Mg and Fe simply assuming that these errors are uncorrelated. In reality, these errors are likely to be correlated, and uncertainty for Mg # would be correspondingly smaller.

[d]Note that this Mg # and its uncertainty are the assumption made for the composition model of *Palme and O'Neill* [2003]. See text for discussion.

concentrations in our model are almost identical to the previous estimates. Since Mg, Si and Fe oxides contribute more than 90% to the mass of the bulk silicate Earth, our model of Earth's composition is indistinguishable from the previous models regarding its implications for the bulk Earth's mineral composition and seismological data. Similarly to the previous models, Mg/Si ratio is superchondritic, which might be due to preaccretional volatilization of silicon from the inner solar system (Mg and Si have lower condensation temperatures than RLE), or partitioning of silicon into Earth's core [e.g., *Palme and O'Neill*, 2003, and references therein].

[52] The most important feature of the new BSE model is its relative depletion in refractory elements compared to previous estimates. In models by *Hart and Zindler* [1986], *McDonough and Sun* [1995], and *Palme and O'Neill* [2003] the predicted RLE enrichment factor is between 2.5 and 2.8. In the new model presented here, the enrichment factor is noticeably lower, with the median value around 2.16. The ∼20% difference between our estimate of the enrichment factor and the commonly used one by McDonough and Sun corresponds to up to 20% lower abundances of refractory elements in the bulk silicate Earth. This depletion is further amplified for the concentrations of incompatible RLEs in the present-day mantle (i.e., Earth's mantle after the extraction of the continental crust). The present-day mantle composition can be derived as the PM composition minus the composition of continental crust, the latter of which is highly enriched in incompatible elements. The average composition of continental crust is constrained by the composition of continental rocks, and is thus entirely independent from our estimate of BSE composition. Therefore our low estimate of the enrichment factor results in up to 60% depletion of incompatible RLEs in the present-day mantle. The detailed discussion on the present-day mantle

composition inferred from our PM model, as well as its implications on mantle structure and evolution, is given in our companion paper.

[53] The new results for the enrichment factor not only affect the abundances of refractory lithophile elements in the bulk silicate Earth and the present-day mantle. The PM abundances of many nonrefractory elements are derived through the bulk Earth ratios with refractory elements. The most prominent example is the PM concentration of K, which is estimated based on the bulk Earth K/U and K/La ratios [*McDonough and Sun*, 1995; *Palme and O'Neill*, 2003]. Similarly, the enrichment factor is used in estimating the PM concentrations of Rb, Ba, As, Mo, Bi, etc. (Table 3). Moreover, some of these abundances of nonrefractory elements are further used to derive the bulk silicate Earth concentrations of yet other elements, such as halogens, B, Sb and Tl. Therefore we revise the PM concentrations of all the chemical elements that are modeled, directly or indirectly, via the RLE enrichment factor; the details of these derivations are given in sections 4.1–4.3.

[54] The PM abundances of highly siderophile elements Ru, Rh, Pd, Os, Pt, and Au are derived through the chondritic ratios with Ir [*Palme and O'Neill*, 2003], which has a rather uniform distribution in mantle peridotites [*Morgan et al.*, 2001]. The PM abundance of Re is further found from the chondritic ratio with Os [*Palme and O'Neill*, 2003]. As our revised estimates for the enrichment factor does not affect this derivation, we adopt the values for all of those siderophile elements from the literature [*Palme and O'Neill*, 2003] (Table 3). We do not consider the atmophile elements (H, C, O, and N), because the estimate of their PM abundances heavily depends on the assumed degassing history [e.g., *Zhang and Zindler*, 1993; *Palme and O'Neill*, 2003].

Table 3. Composition of Earth's Primitive Mantle

Z	Element	CI[a]	PM[b]	SD[c]	Constraints	Reference
3	Li, ppm	1.5	1.6	0.4	Peridotite compositions [McDonough and Sun, 1995; Palme and O'Neill, 2003]	
4	Be, ppb	25	54.0	9.2	RLE enrichment factor	this work
5	B, ppm	0.87	0.17	0.08	B/K ~ 0.0010(3); B/Rb = 0.4(1) [Chaussidon and Jambon, 1994]	this work
9	F, ppm	60	18	8	F/K ~ 0.09(4); F/P ~ 0.3(1) [Schilling et al., 1980; Smith et al., 1981]	this work
11	Na, ppm	5,000	2,220	1,050	PCA, Bootstrap	this work
12	Mg, %	9.70	23.41	0.93	PCA, Bootstrap	this work
13	Al, %	0.865	1.87	0.32	PCA, Bootstrap	this work
14	Si, %	10.64	21.09	0.58	PCA, Bootstrap	this work
15	P, ppm	950	66	15	Ti/P ~ 13.7; P/Nd ~ 65(10) [Sun, 1982; McDonough et al., 1985; Langmuir et al., 1992]	this work
16	S, ppm	54,100	230	80	Peridotite and komatiite compositions	O'Neill [1991] and McDonough and Sun [1995]
17	Cl, ppm	700	1.4	0.5	Cl/K ~ 0.0075(25) [Saal et al., 2002]	this work
19	K, ppm	550	190	40	K/U ~ 10,000–12,700; K/La ~ 340(20) [Wasserburg et al., 1964; Schilling et al., 1980]	this work
20	Ca, %	0.926	2.00	0.34	PCA, Bootstrap	this work
21	Sc, ppm	5.9	12.7	2.2	PCA, Bootstrap	this work
22	Ti, ppm	440	950	163	PCA, Bootstrap	this work
23	V, ppm	55	74	12	PCA, Bootstrap	this work
24	Cr, ppm	2,650	2,645	390	PCA, Bootstrap	this work
25	Mn, ppm	1,940	1,020	90	PCA, Bootstrap	this work
26	Fe, %	18.20	6.22	0.42	PCA, Bootstrap	this work
27	Co, ppm	505	105	8	PCA, Bootstrap	this work
28	Ni, ppm	11,000	1,985	215	PCA, Bootstrap	this work
29	Cu, ppm	125	25	10	Peridotite, komatiite and MORB compositions	Sun [1982], O'Neill [1991], and, McDonough and Sun [1995]
30	Zn, ppm	315	58	17	PCA, Bootstrap	this work
31	Ga, ppm	9.8	4.2	0.4	Peridotite and basalt compositions	McDonough and Sun [1995] and O'Neill and Palme [1998]
32	Ge, ppm	33	1.15	0.25	Peridotite composition	McDonough and Sun [1995] and O'Neill and Palme [1998]
33	As, ppm	1.85	0.050	0.035	As/Ce ~ 0.037(25) [Sims et al., 1990]	this work
34	Se, ppm	21	0.075	0.050	Peridotite compositions, Se/S in chondrites	McDonough and Sun [1995]
35	Br, ppb	3.5	3.6	0.4	Cl/Br ~ 400(50) [Schilling et al., 1980; Jambon et al., 1995]	this work
37	Rb, ppm	2.3	0.457	0.084	Rb/Sr ~ 0.029(2); Rb/Ba ~ 0.09(2) [Hofmann and White, 1983; McDonough et al., 1992]	this work
38	Sr, ppm	7.3	15.8	2.7	RLE enrichment factor	this work
39	Y, ppm	1.56	3.37	0.58	RLE enrichment factor	this work
40	Zr, ppm	3.9	8.42	1.44	RLE enrichment factor	this work
41	Nb, ppb	250	460	170	RLE enrichment factor	this work
42	Mo, ppb	920	30	17	Mo/Ce ~ 0.027(12); Mo/Nb ~ 0.050(15) [Sims et al., 1990]	this work
44	Ru, ppb	710	5	1.5	Ru/Ir in CI chondrite	Palme and O'Neill [2003]
45	Rh, ppb	140	0.9	0.3	Rh/Ir in CI chondrite	Palme and O'Neill [2003]
46	Pd, ppb	560	3.6	2.8	Pd/Ir in H chondrite	Palme and O'Neill [2003]
47	Ag, ppb	200	4	u	Peridotite compositions, Ag/Na in bulk Earth	Sun [1982], McDonough and Sun [1995], Palme and O'Neill [2003]
48	Cd, ppb	690	50	u	Peridotite and komatiite compositions, Zn/Cd in bulk Earth	McDonough and Sun [1995] and Palme and O'Neill [2003]
49	In, ppb	80	10.1	3.8	In/Y ~ 0.003(1) [Yi et al., 1995]	this work
50	Sn, ppb	1,700	103	26	Sn/Sm ~ 0.32(6) [Jochum et al., 1993]	this work
51	Sb, ppb	135	7	4	Sb/Pb ~ 0.074(31); Sb/Ce ~ 0.003; Sb/Pr ~ 0.35(15) [Sims et al., 1990; Jochum and Hofmann, 1997]	this work
52	Te, ppb	2,300	8	u	Peridotite compositions	Palme and O'Neill [2003]
53	I, ppb	430	10	u	Peridotite and basalt compositions	Deruelle et al. [1992]
55	Cs, ppb	190	16	6	Rb/Cs ~ 28(10) [McDonough et al., 1992]	this work
56	Ba, ppm	2.35	5.08	0.87	RLE enrichment factor	this work
57	La, ppb	235	508	87	PCA, Bootstrap	this work

Table 3. (continued)

Z	Element	CI[a]	PM[b]	SD[c]	Constraints	Reference
58	Ce, ppb	620	1340	230	PCA, Bootstrap	this work
59	Pr, ppb	94	203	35	RLE enrichment factor	this work
60	Nd, ppb	460	994	170	PCA, Bootstrap	this work
62	Sm, ppb	150	324	55	PCA, Bootstrap	this work
63	Eu, ppb	57	123	21	PCA, Bootstrap	this work
64	Gd, ppb	200	432	74	RLE enrichment factor	this work
65	Tb, ppb	37	80	14	PCA, Bootstrap	this work
66	Dy, ppb	250	540	92	RLE enrichment factor	this work
67	Ho, ppb	56	121	21	RLE enrichment factor	this work
68	Er, ppb	160	346	59	RLE enrichment factor	this work
69	Tm, ppb	25	54.0	9.2	RLE enrichment factor	this work
70	Yb, ppb	160	346	59	PCA, Bootstrap	this work
71	Lu, ppb	25	54.0	9.2	PCA, Bootstrap	this work
72	Hf, ppb	105	227	39	RLE enrichment factor	this work
73	Ta, ppb	14	30.2	5.2	RLE enrichment factor	this work
74	W, ppb	93	11.9	2.8	W/Th $\sim$ 0.19(3) [*Newsom et al.*, 1996]	this work
75	Re, ppb	38	0.32	0.3	Re/Ir in H chondrite	*Palme and O'Neill* [2003]
76	Os, ppb	490	3.4	0.34	Os/Ir in H chondrite	*Palme and O'Neill* [2003]
77	Ir, ppb	465	3.2	0.2	Peridotite compositions	*Morgan et al.* [2001]
78	Pt, ppb	1000	6.6	0.8	Pt/Ir in CI chondrite	*Palme and O'Neill* [2003]
79	Au, ppb	145	0.88	0.10	Ir/Au in H chondrite	*Palme and O'Neill* [2003]
80	Hg, ppb	310	6	u	Peridotite and basalt compositions, Hg/Se in continental crust	*Palme and O'Neill* [2003]
82	Tl, ppb	142	2	u	Tl/Rb $\sim$ 0.005 [*Hertogen et al.*, 1980; *Palme and O'Neill*, 2003]	this work
82	Pb, ppb	2,530	144	26	^{238}U/^{204}Pb $\sim$ 8.5(5) [*Stacey and Kramers*, 1975; *Sun*, 1982]	this work
83	Bi, ppb	110	4	u	Bi/La $\sim$ 0.008 [*Palme and O'Neill*, 2003]	this work
90	Th, ppb	29	62.6	10.7	RLE enrichment factor	this work
92	U, ppb	8	17.3	3.0	RLE enrichment factor	this work

[a]CI composition according to Lodders and Fegley [1998].
[b]Primitive mantle composition derived in this study.
[c]One standard deviation from the median; "u" denotes undefined uncertainty.

4.1. Refractory Lithophile Elements: Derivation via the Enrichment Factor

[55] The new estimate of the RLE enrichment factor is based on the derived PM abundances of 12 different RLEs with different compatibilities during mantle melting. The enrichment factor also determines the concentration of other RLEs (e.g., U, Th, Ta), which do not have a sufficiently large number of measurements required for our statistical analysis. The uncertainty of these estimates is determined by the uncertainty of the enrichment factor ($\sim$17%, Table 2). This limited accuracy in our knowledge of Earth's abundance of refractory elements (including heat-producing elements U and Th) has important implications, although this issue has rarely been emphasized in literature.

[56] Although Nb is usually regarded refractory and lithophile, it may develop a siderophile behavior in high-pressure conditions [*Wade and Wood*, 2001]. Core extraction thus may have affected the absolute abundance of Nb in the primitive mantle. Similar to *Palme and O'Neill* [2003], we adopt $\sim$15% lower value of Nb abundance in the primitive mantle compared to other RLEs, but with higher uncertainty because this issue is still controversial.

4.2. Nonrefractory Elements: Direct Derivation

[57] For a number of nonrefractory elements, their PM abundances have been derived based on the analysis of mantle peridotite compositions: for elements with approximately constant concentrations in peridotites their PM abundance is believed to be close to the peridotite abundance (e.g., Li, Zn, Se, Te, Ir [e.g., *Jagoutz et al.*, 1979; *Sun*, 1982; *McDonough and Sun*, 1995; *Morgan et al.*, 2001]). Additionally, analysis of komatiite and basalt compositions can be used to assess the solid-melt distribution coefficient for these elements and correct for the effects of melting (e.g., S, Gu, Ga [e.g., *Sun*, 1982; *O'Neill*, 1991; *McDonough and Sun*, 1995]). Alternatively, if the ratio of two elements is relatively constant in mantle peridotites worldwide, this ratio can be used to infer the PM abundance of one of the elements, if the PM abundance of the other element is already established. The most frequently used ratios are Mg/Ni, Fe/Mn, Ti/Na, and Ni/Co [*McDonough and Sun*, 1995]. Another way to determine the PM abundances of nonrefractory elements involves correlations with Mg or Si in peridotite data space (e.g., V, Cr, Ga) [*Palme and O'Neill*, 2003].

[58] As all of these methods are based on the correlations of element abundances in peridotite data, they are already incorporated in our statistical analysis. Therefore we directly derive the PM abundances of ten nonrefractory elements: lithophiles (Si,Mg,Cr,Mn), siderophiles (Fe,Ni,Co,V), and volatiles (Na,Zn). In all cases, our results for these elements are indistinguishable (within uncertainty) from the previous estimates. The new method is, however, preferable, since it allows us to determine the PM abundances of a number of refractory and nonrefractory elements simultaneously, and to accurately propagate the uncertainty into the final result,

taking into account the scatters in peridotite data. For elements with too few measurements (S, Li, Cu, Ge, Ga, Se, and Ir), we adopt their values from the literature (Table 3).

[59] For most of the nonrefractory elements, their uncertainty is in the range of 5 to 20%. Smaller uncertainty for Si (~3%) is explained by its almost constant content in fertile mantle peridotites. Larger uncertainties for Zn (30%) and Na (50%) arise from high scatters in their concentrations in the data set used for this study.

4.3. Nonrefractory Elements: Derivation via Bulk Earth Ratios

[60] Another approach to deriving the PM concentration of the nonrefractory elements utilizes the so-called bulk Earth ratios with other elements, for which their PM concentrations are already determined. Those bulk Earth ratios are, of course, unknown. However, the chemical elements with similar incompatibility during mantle melting are expected to retain their bulk Earth ratio during crust-mantle differentiation. The continental crust and the mid-ocean ridge basalt (MORB) source mantle are believed to be complementary reservoirs [e.g., *Hofmann*, 1988]. Therefore, if a similar value is observed for a particular ratio in both continental crust and MORB, it is assumed that the bulk Earth ratio is somewhere between these crustal and MORB values. Although this method is relatively imprecise due to large scatters in the compositional data of ocean basalts and even larger scatters in those of continental rocks, for elements such as K, Rb, Cs, Sn, and some others, this is the only way to determine their PM abundance.

[61] If the PM abundance of an element is derived through the bulk Earth ratio with a refractory lithophile element, it is also a function of the RLE enrichment factor. Therefore the new estimate of the enrichment factor derived here implies ~20% lower PM concentrations of all such elements, compared to the previous models. At the same time, the uncertainty of those estimates is fairly high as it is affected by the uncertainties for the RLE enrichment factor as well as the bulk Earth ratio. This is the case for the following elements: K, P, As, Rb, Mo, Sn, Cs, In, W, Pb and Bi (Table 3). Of these, potassium is probably the most important in geophysical and geochemical modeling, as it is both the heat-producing element and the parental element for ^{40}Ar, which plays a key role in our understanding of Earth's degassing history. Therefore we will discuss the derivation of K abundance in the primitive mantle in some details below.

[62] The K abundance in the primitive mantle can be derived through the bulk K/U ratio, which is in the vicinity of 10,000 for most of continental rocks [*Wasserburg et al.*, 1964], and is relatively constant at $12,700 \pm 200$ in the normal-type mid-ocean ridge basalts (MORB) [*Jochum et al.*, 1983]. As U is slightly more incompatible than K during mantle melting, the MORB source mantle (i.e., the residual mantle after the extraction of continental crust) is expected to have a slightly higher K/U ratio compared to the bulk Earth ratio. Therefore K estimates inferred from K/U ratios in MORB and in the continental crust are respectively the upper and the lower bounds of the PM potassium concentration. A recent study by *Lassiter* [2004] suggests that the bulk Earth K/U ratio may be as low as 7000 due to unaccounted remnants of recycled oceanic crust with very

low K content. Although it is a plausible scenario, the amount of stored subducted crust in the present-day convecting mantle is hard to quantify, and the estimate of the bulk K/U becomes very uncertain. We will thus adopt a conservative range for the bulk Earth K/U ratio. Given our new estimate of U abundance, the PM concentration of K then falls somewhere between 173 ± 30 ppm and 219 ± 38 ppm.

[63] Another constraint on the K abundance in the PM comes from K/La ratio, which is relatively constant at about 330 in MORB [*Schilling et al.*, 1980], in oceanic island basalts (OIB) and continental flood basalts, but is somewhat higher in the continental crust [*O'Neill and Palme*, 1998]. In contrast to U, La is slightly more compatible than K during mantle melting [*O'Neill and Palme*, 1998], and the K abundance of 168 ± 32 derived from K/La ~ 330 ± 30 is thus the lower bound of the estimate. We follow the approach by *O'Neill and Palme* [1998] and *Palme and O'Neill* [2003] and adopt the mean value of the two estimates, 168 ± 32 from K/La in MORB, and 219 ± 38 ppm from K/U in MORB, to arrive at 190 ± 40 ppm for the concentration of K in the primitive mantle.

[64] The derivation of the primitive mantle abundances of other elements, based on their bulk Earth ratios with RLEs, is analogous to that for K. When two constraints are available, we choose the mean value of the two estimates; the uncertainty is calculated based on uncertainties of the RLE enrichment factor and the bulk Earth ratio. The abundances of some of these elements (e.g., K, Rb) are further used to derive the PM abundances of yet other nonrefractory elements (e.g., B, F, Cl, Br, Sb, Tl, Table 3). The uncertainty of those estimates is further amplified, in some cases exceeding 50%.

5. Discussion
5.1. Comparison With Previous Models

[65] Compared to our model, the previous models of the primitive mantle favor a higher RLE enrichment factor: ~2.5 in the models by *Jagoutz et al.* [1979] and *Hart and Zindler* [1986], 2.75 ~ 2.8 in the models by *McDonough and Sun* [1995] and *Palme and O'Neill* [2003]. Given reported uncertainty, some of earlier estimates overlap with ours (e.g., 2.51 ± 0.25 [*Hart and Zindler*, 1986] and 2.16 ± 0.37 of this study), but an important point is that the mean value is lowered. With the model of *Hart and Zindler* [1986], for example, one may have to be at the edge of the confidence limit to use the enrichment factor of 2.25, but this value is now near the maximum of the probability distribution (Figure 8d). The discrepancy between our model and previous models is not surprising in the view of highly scattered compositional data of mantle peridotites, with trace elements concentrations varying by several orders of magnitude. Figure 9 shows the distribution of the average RLE enrichment factor calculated for the peridotite samples used in this study. Although for most of the samples the average enrichment factor is close to 2.0, the deviations of individual enrichment factors (corresponding to different RLEs) are above 15%, and in some cases exceed an order of magnitude. Clearly, none of those samples can be regarded as primitive (with regard to the chondritic constraints). We need a careful statistical treatment in order to extract
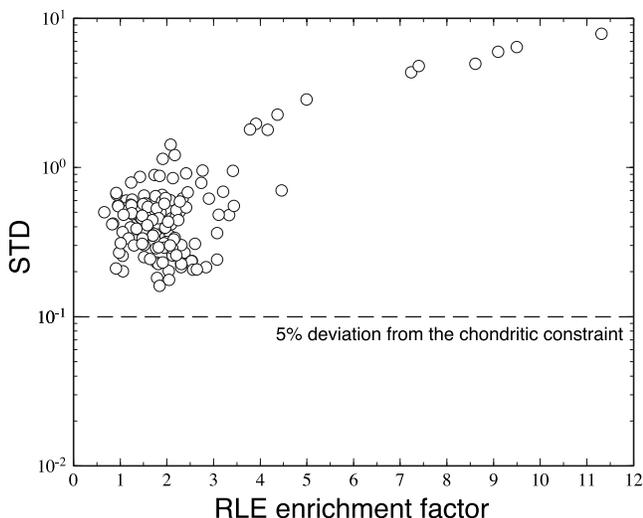
Figure 9. Average RLE enrichment factor versus standard deviation of individual enrichment factors (Ca, Al, Ti, Nd, Sm, Eu, Yb) from their average for peridotite samples used in this study. The dashed line shows the maximum standard deviation (0.1) for the RLE enrichment factor allowed in our stochastic inversion. This criterion corresponds to up to 5% deviation from the chondritic constraints when the enrichment factor is 2.0.

compositional trends from noisy peridotite data and apply cosmochemical constraints.

[66] The most recent model by *Palme and O'Neill* [2003] is characterized by the highest value for the RLE enrichment factor, 2.8 ± 0.2, and this requires some explanation. This model is based on a method first introduced by *O'Neill and Palme* [1998], which involves the mass balance of major oxides MgO, SiO$_2$, FeO, CaO and Al$_2$O$_3$ in Earth's

mantle. The procedure for deriving the RLE enrichment factor is the following. First, the value of Mg # in Earth's primitive mantle is assumed, and combined with the average FeO composition in the most fertile peridotites, the MgO abundance is derived from this Mg #. On the next step, the PM value of SiO$_2$ is determined through linear correlation with MgO. Finally, the PM concentration of Al$_2$O$_3$ is derived from the chondritic Ca/Al ratio and the closure property (i.e., $\sim$98.41 wt % for the sum of the five major oxides). Although this method may have an advantage of relying exclusively on major element concentrations for deriving the PM composition, it also requires more assumptions compared to the more common pyrolite-type approach. In particular, in addition to using the peridotite melting trend (SiO$_2$ versus MgO) and the chondritic constraint (Ca/Al), this method has to assume Mg # and FeO abundance in the primitive mantle.

[67] The estimate of the RLE enrichment factor based on this method is highly unstable, being very sensitive to the assumed values of Mg# and FeO content of the primitive mantle (Figure 10). By choosing Mg # = 89.0 ± 0.1 and Fe = 8.1 ± 0.05 wt % [*Palme and O'Neill*, 2003] obtained the estimate of the RLE enrichment factor $\sim$2.8 $\pm$ 0.22. However, the range of Mg # in fertile peridotites (with MgO < 39%) is about 88.0$\sim$90.0. Assuming only 0.5% higher Mg # (i.e., 89.4 instead of 89.0) will result in >20% lower enrichment factor (2.2 instead of 2.8, Figure 10). In fact, repeating those calculations, with our new estimates of FeO and Mg # in the primitive mantle, yields a value of RLE enrichment factor almost identical to our estimate based on PCA and bootstrap technique. This demonstrates the internal consistency of our new model in terms of the mass balance of major oxides. At the same time, the mass balance method for deriving the primitive mantle composition turns to be of only limited use as it requires the precise knowledge of the primitive Mg # and FeO content, which should
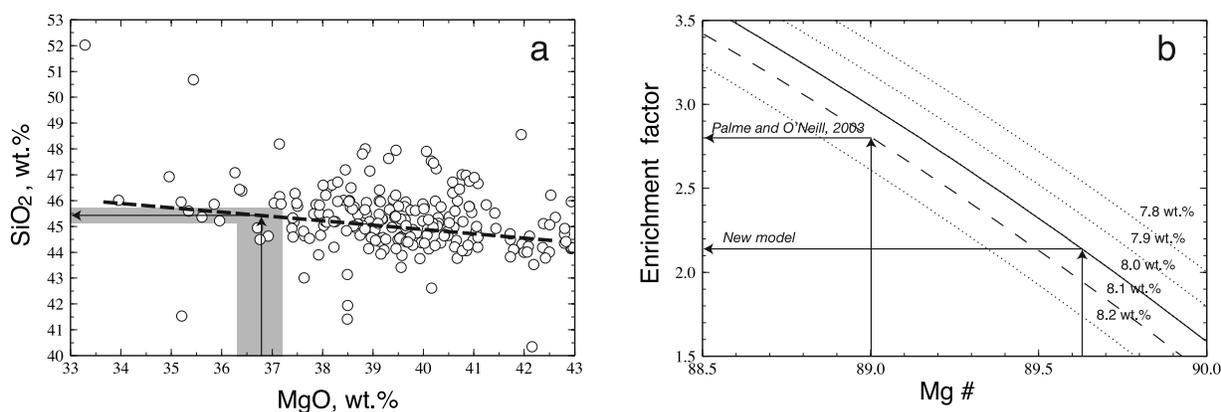
Figure 10. Derivation of the RLE enrichment factor in the model by *Palme and O'Neill* [2003]. (a) Derivation of PM abundance of SiO$_2$ from the melting trend in Mg versus Si space. Shaded regions denote the reported uncertainty in the model by *Palme and O'Neill* [2003]. (b) RLE enrichment factor as a function of Mg # for different FeO abundances assumed for the primitive mantle. Dashed curve corresponds to the preferred FeO value in the model by *Palme and O'Neill* [2003]; solid curve corresponds to the FeO abundance derived in this paper. The RLE enrichment factor (for Al) is derived based on the assumed values of Mg # and FeO abundance in the primitive mantle. The RLE enrichment factor is $\sim$2.8 for Mg # $\sim$89.0 and FeO $\sim$ 8.1% [*Palme and O'Neill*, 2003], and is $\sim$2.16 for Mg # $\sim$ 89.6 and FeO $\sim$ 8.0% (this study).

be the output, not the input, of geochemical inference on BSE composition.

5.2. The cpx Correction

[68] The cpx correction was proposed by *Hart and Zindler* [1986] as a way to fix the peridotite compositions distorted by local cpx heterogeneities, which are thought to cause the superchondritic Ca/Al ratios in peridotite samples. On the contrary, *McDonough and Sun* [1995] claim that the elevated Ca/Al ratios are likely to result from melt depletion processes in the mantle, and no correction is needed to arrive at chondritic Ca/Al values in the primitive mantle by modeling melting trends in peridotites.

[69] We try to resolve this problem by constructing the primitive mantle model for both the raw data and the cpx-corrected data. Following *Hart and Zindler* [1986], we correct the peridotite compositions by subtracting small amounts of cpx until the Ca/Al ratio is lowered to the chondritic level ($\sim$1.1). We use the spinel lherzolite norm by *Kelemen et al.* [1992] for calculating mineral modes in mantle peridotites from their bulk compositions for Si, Mg, Fe, Al, Ca, Na, K and Cr. The abundance of Ti as well as other trace elements in mantle minerals are determined from the partition coefficients compiled by *Bedard* [1994]. In different subsets used for this study, up to 70% of the peridotite compositions were corrected, with the average amount of cpx subtracted around 17%.

[70] The results for the cpx-corrected data set are barely distinguishable from those derived for the raw data (Table 1). The primitive mantle composition determined from the cpx-corrected data set is characterized by slightly lower RLE enrichment factor and slightly higher Mg abundance; these differences are, however, within the uncertainty of our model. Regardless of cpx correction, our PM models have chondritic RLE ratios (including Ca/Al), since in our method we accept only those PM compositions that have RLE ratios within 5% of the CI value. However, for the raw data set, the number of bootstrap ensembles that we need to compute in order to collect 10^4 acceptable solutions (i.e., those with chondritic RLE ratios), is in some cases $\sim$50% larger than for the cpx-corrected data set. Still, the elevated Ca/Al ratios in the raw data set do not prevent us from constructing the "chondritic" primitive mantle composition. Therefore, as *McDonough and Sun* [1995] suggested, the superchondritic Ca/Al in mantle peridotites can be attributed to melting processes, if large scatters in Ca and Al concentrations are taken into account. At the same time, even though cpx correction did not play a vital role in our method as far as the final result is concerned, it is still important to bear in mind the possibility of excess cpx in natural peridotite samples. The CaO and Al_2O_3 contents of our PM model are lower than those of some of the fertile peridotites typically used in mantle melting experiments. As Figure 10 demonstrates, our estimate on CaO and Al_2O_3 in the primitive mantle can be regarded as a direct consequence of imposing the chondritic Ca/Al and Mg # of 89.6 on the simple major oxide mass balance. Fertile peridotites enriched in CaO and Al_2O_3 compared to our PM model may thus contain excess cpx. For example, spinel peridotite KLB-1 used in a number of melting experiments has superchondritic Ca/Al of $\sim$1.3 [*Takahashi*, 1986], which may be indicative of cpx enrichment.

[71] In some of previous PM models the high Ca/Al ratios in peridotites were used to argue for the superchondritic value of Ca/Al in the primitive (upper) mantle [e.g., *Ringwood*, 1975; *Jagoutz et al.*, 1979; *Wänke*, 1981]. To reconcile it with the postulated chondritic Ca/Al ratio for the bulk Earth, the subchondritic Ca/Al in some hidden parts of the mantle must be assumed. Fractionation in deep magma ocean may have led to the segregation of $10-15\%$ of Mg- and Ca-perovskite assemblage in the deep mantle, which led to superchondritic Ca/Al in convecting mantle [e.g., *Walter and Trønnes*, 2004, and references therein]. However, our results suggest that the superchondritic Ca/Al ratio is not an original feature of Earth's upper mantle as a whole, but rather the result of melting processes, with some contributions from modal heterogeneity in mantle rocks. Although slight deviations from the strictly chondritic Ca/Al ratio in the upper mantle are hard to rule out, due to the large uncertainties associated with compositional trends, there seems to be no evidence for a significant violation of the chondritic constraint in the primitive mantle RLE ratios.

6. Conclusions

[72] The new statistical approach presented here allows us to avoid most of the difficulties inherent in the pyrolite-type approach for deriving the PM composition. We model the peridotite melting trend in multidimensional space by principal component analysis. The nonlinearity of the melting trend is handled by modeling in the logarithmic space. The primitive mantle composition is located on the melting trend by simultaneously imposing multiple chondritic constraints (i.e., the chondritic values for the bulk Earth RLE ratios) with least squares. Finally, we use the bootstrap resampling technique to directly map scatters in peridotite data into the variance of the PM model. Our resulting PM model is similar to the previous models in terms of Mg, Si and Fe abundances, but it is depleted in some major (Al, Ca, Ti) and a number of trace elements (REE, Zr, Rb, etc.), as the RLE enrichment factor is found to be $\sim$20% lower compared to the previous estimates ($\sim$2.16 $\pm$ 0.37). For highly incompatible elements (e.g., light REE and the heat-producing elements K, U, and Th) the depletion is further amplified in the present-day mantle composition, which may exceed 50% compared to the previous estimates.

Appendix A: Principal Component Analysis

[73] To set up the notation, we start with a brief review of mathematical principles behind PCA. We may express the lognormalized data set $\{p_i^j\}$ (equation (3)) as an $n \times m$ matrix,

$$P = \begin{bmatrix} p_1^1 & p_2^1 & \cdots & p_m^1 \\ p_1^2 & p_2^2 & \cdots & p_m^2 \\ \vdots & \vdots & \ddots & \vdots \\ p_1^n & p_2^n & \cdots & p_m^n \end{bmatrix}, \qquad (A1)$$

and because of equation (5), the covariance matrix of $\{p_i^j\}$ can readily be calculated from P as $C_P = P^T P$, where the

superscript T denotes transpose. The covariance matrix is semipositive definite, so all of its eigenvalues are nonnegative real numbers. We can thus always decompose the covariance matrix as

$$C_P = A^T \cdot \text{diag}\{\lambda_1 \cdots \lambda_m\} \cdot A, \tag{A2}$$

where eigenvalues λ_i are ordered such that

$$\lambda_1 \geq \lambda_2 \geq .. \geq \lambda_m \geq 0, \tag{A3}$$

and corresponding eigenvectors $\mathbf{a_i}$ are collectively denoted by

$$A = [\mathbf{a_1}\, \mathbf{a_2}\, \cdots\, \mathbf{a_m}]. \tag{A4}$$

[74] The matrix A is orthonormal (i.e., $A^T A = I$), and its geometrical meaning is rotation in the m-dimensional space. If we denote the representation of $\{p_i^j\}$ in the new coordinate system created by this rotation as $\{q_i^j\}$ and the corresponding matrix as Q, the following relation holds:

$$Q = PA. \tag{A5}$$

The covariance matrix is now

$$C_Q = Q^T Q = (PA)^T PA = A^T C_P A = \text{diag}\{\lambda_1 \cdots \lambda_m\}. \tag{A6}$$

That is, $\Sigma_j (q_i^j)^2 = \lambda_i$, and the covariance of q_i and q_j exactly vanishes in this rotated coordinate system.

[75] When the first eigenvalue is dominant ($\lambda_1 \gg \lambda_2$), the overall structure of $\{p_i^j\}$ may be well represented by the first principal component $\{q_1^j\}$. We denote this component by a vector $\mathbf{q_1}$, and from equation (A5), we can see that

$$\mathbf{q_1} = P\mathbf{a_1}, \tag{A7}$$

or more explicitly with $\mathbf{a_1} = [a_1 a_2 \cdots a_m]^T$

$$q_1^j = a_1 p_1^j + a_2 p_2^j + \cdots + a_m p_m^j. \tag{A8}$$

This is the same as equation (6). In the main text, q_1^j is simply denoted as q^j. The first principal component (and any other principal components) is simply a weighted sum of the original concentration data. Note that the coefficients a_i provided by PCA are already normalized so that $\Sigma_i (a_i)^2 = 1$.

[76] An expression for the part of the original data explained by the first principal component may be derived as follows. We can isolate the first principal component by constructing the following matrix:

$$\widetilde{Q} = [\mathbf{q_1}\, \underbrace{\mathbf{0} \cdots \mathbf{0}}_{m-1}]. \tag{A9}$$

The corresponding representation in the original coordinates is then given by

$$\widetilde{P} = \widetilde{Q}A^{-1} = \widetilde{Q}A^T. \tag{A10}$$

This is equivalent to equation (7).

References

Albarède, F. (1996), *Introduction to Geochemical Modeling*, Cambridge Univ. Press, New York.

Allègre, C., A. Hofmann, and K. O'Nions (1996), The argon constraints on mantle structure, *Geophys. Res. Lett.*, 23, 3555–3557.

Allègre, C., G. Manhes, and E. Lewin (2001), Chemical composition of the Earth and the volatility control on planetary genetics, *Earth Planet. Sci. Lett.*, 185, 49–69.

Allègre, C. J., J.-P. Poirier, E. Humler, and A. Hofmann (1995), The chemical composition of the Earth, *Earth Planet. Sci. Lett.*, 96, 61–88.

Anderson, D. L. (1983), Chemical composition of the mantle, *Proc. Lunar Planet. Sci. Conf. 14th*, Part 1, *J. Geophys. Res.*, 88, suppl., B41–B52.

Anderson, D. L. (1989), *Theory of the Earth*, Blackwell Sci., Malden, Mass.

Bedard, J. H. (1994), A procedure for calculating the equilibrium distribution of trace elements among the mineral cumulate rocks, and the concentration of trace elements in coexisting liquids, *Chem. Geol.*, 118, 143–153.

Blichert-Toft, J., and F. Albarède (1997), The Lu-Hf isotope geochemistry of chondrites and the evolution of the mantle-crust system, *Earth Planet. Sci. Lett.*, 148, 243–258.

Boyd, F. R. (1989), Compositional distinction between oceanic and cratonic lithosphere, *Earth Planet. Sci. Lett.*, 96, 15–26.

Boyet, M., and R. W. Carlson (2005), ^{142}Nd evidence for early (4.53 Ga) global differentiation of the silicate Earth, *Science*, 309, 576–581.

Chaussidon, M., and A. Jambon (1994), Boron content and isotopic composition of oceanic basalts: geochemical and cosmochemical implications, *Earth Planet. Sci. Lett.*, 121, 277–291.

Clayton, R. N., and T. K. Mayeda (1996), Oxygen isotope studies of achondrites, *Geochim. Cosmochim. Acta*, 60, 1999–2017.

Davis, A. M., and F. M. Richter (2003), Condensation and evaporation of solar system materials, in *Treatise on Geochemistry*, vol. 1, edited by H. Holland and K. K. Turekian, pp. 407–430, Elsevier, New York.

DePaolo, D. J., and G. J. Wasserburg (1976), Nd isotopic variations and petrogenetic models, *Geophys. Res. Lett.*, 3, 249–252.

Deruelle, B., G. Dreibus, and A. Jambon (1992), Iodine abundances in oceanic basalts: Implications for Earth dynamics, *Earth Planet. Sci. Lett.*, 108, 217–227.

Drake, M. J., and K. Righter (2002), Determining the composition of the Earth, *Nature*, 416, 39–44.

Fukao, Y., S. Widiyantoro, and M. Obayashi (2001), Stagnant slabs in the upper and lower mantle transition region, *Rev. Geophys.*, 39, 291–323.

Gast, P. W. (1960), Limitations on the composition of the upper mantle, *J. Geophys. Res.*, 65, 1287–1297.

Gershenfeld, N. (1998), *The Nature of Mathematical Modeling*, Cambridge Univ. Press, New York.

Hager, B. H., R. W. Clayton, M. A. Richards, R. P. Comer, and A. M. Dziewonski (1985), Lower mantle heterogeneity, dynamic topography and the geoid, *Nature*, 313, 541–545.

Hart, S. R., and A. Zindler (1986), In search of a bulk-Earth composition, *Chem. Geol.*, 57, 247–267.

Hertogen, J., M.-J. Janssens, and H. Palme (1980), Trace elements in ocean ridge basalt glasses: Implications for fractionations during mantle evolution and petrogenesis, *Geochim. Cosmochim. Acta*, 44, 2125–2143.

Hofmann, A. W. (1988), Chemical differentiation of the Earh: the relationship between mantle, continental crust, and oceanic crust, *Earth Planet. Sci. Lett.*, 90, 297–314.

Hofmann, A. W., and W. M. White (1983), Ba, Rb and Cs in the Earth's mantle, *Z. Naturforsch.*, 38a, 256–266.

Irving, A. J. (1980), Petrology and geochemistry of composite ultramafic xenoliths in alkalic basalts and implications for magmatic processes within the mantle, *Am. J. Sci.*, 280A, 389–426.

Jagoutz, E., H. Palme, H. Baddenhausen, K. Blum, M. Cendales, G. Dreibus, B. Spettel, V. Lorenz, and H. Wänke (1979), The abundances of major, minor and trace elements in the earth's mantle as derived from primitive ultramafic nodules, *Proc. Lunar Planet. Sci. Conf.*, 10th, 2031–2050.

Jambon, A., B. Deruelle, G. Dreibus, and F. Pineau (1995), Chlorine and bromine abundance in MORB: The contrasting behaviour of the Mid-Atlantic Ridge and East-Pacific Rise and implications for chlorine geodynamic cycle, *Chem. Geol.*, 126, 101–117.

Javoy, M. (1995), The integral enstatite chondrite model of the Earth, *Geophys. Res. Lett.*, 22, 2219–2222.

Jochum, K. P., and A. W. Hofmann (1997), Constraints on Earth evolution from antimony in mantle-derived rocks, *Chem. Geol.*, *139*, 39–49.

Jochum, K. P., A. W. Hofmann, E. Ito, H. M. Seufert, and W. M. White (1983), K, U and Th in mid-ocean ridge basalt glasses and heat production, K/U and K/Rb in the mantle, *Nature*, *306*, 431–436.

Jochum, K. P., W. F. McDonough, H. Palme, and B. Spettel (1989), Compositional constraints on continental lithospheric mantle from trace elements in spinel peridotite xenoliths, *Nature*, *340*, 548–550.

Jochum, K. P., A. W. Hofmann, and H. M. Seufert (1993), Tin in the mantle-derived rocks: Constraints on Earth evolution, *Geochim. Cosmochim. Acta*, *57*, 3585–3595.

Kelemen, P. B., H. J. B. Dick, and J. E. Quick (1992), Formation of harzburgite by pervasive melt/rock reaction in the upper mantle, *Nature*, *358*, 635–641.

Kelemen, P. B., S. R. Hart, and S. Bernstein (1998), Silica enrichment in the continental upper mantle via melt/rock reaction, *Earth Planet. Sci. Lett.*, *164*, 387–406.

Kinzler, R. J., and T. L. Grove (1992), Primary magmas of Mid-ocean ridge basalts, 2. Applications, *J. Geophys. Res.*, *97*, 6907–6926.

Klein, E. M., and C. H. Langmuir (1987), Global correlations of ocean ridge basalt chemistry with axial depth and crustal thickness, *J. Geophys. Res.*, *92*, 8089–8115.

Langmuir, C. H., E. M. Klein, and T. Plank (1992), Petrological systematics of mid-ocean ridge basalts: constraints on melt generation beneath ocean ridges, in *Mantle Flow and Melt Generation at Mid-Ocean Ridges*, *Geophys. Monogr. Ser.*, vol. 71, edited by J. Phipps Morgan, D. Blackman, and J. Sinton, pp. 183–280, AGU, Washington, D. C.

Lassiter, J. (2004), The role of recycled oceanic crust in the potassium and argon budget of the Earth: Toward a resolution of the "missing argon" problem, *Geochem. Geophys. Geosyst.*, *5*, Q11012, doi:10.1029/2004GC000711.

Lodders, K. (2003), Solar system abundances and condensation temperatures of the elements, *Astrophys. J.*, *591*, 1220–1247.

Lodders, K., and B. Fegley (1998), *The Planetary Science Companion*, Oxford Univ. Press, New York.

Loubet, M., N. Shimizu, and C. Allègre (1975), Rare Earth elements in Alpine peridotites, *Contrib. Mineral. Petrol.*, *53*, 1–12.

Manson, V. (1967), *Geochemistry of Basaltic Rock: Major Elements. Rare Earth Elements in Alpine Peridotites*, Interscience, Hoboken, N. J.

McBirney, A. R. (1993), *Igneous Petrology*, Jones and Bartlett, Boston, Mass.

McDonough, W., S.-S. Sun, A. E. Ringwood, E. Jagoutz, and A. W. Hofmann (1992), Potassium, rubidium and cesium in the Earth and Moon and the evolution of the mantle of the Earth, *Geochim. Cosmochim. Acta*, *56*, 1001–1012.

McDonough, W. F., and S.-S. Sun (1995), The composition of the Earth, *Chem. Geol.*, *120*, 223–253.

McDonough, W. F., M. T. McCulloch, and S.-S. Sun (1985), Isotopic and geochemical systematics in Tertiary-Recent basalts from southeastern Australia and implications for the evolution of the sub-continental lithosphere, *Geochim. Cosmochim. Acta*, *49*, 2051–2067.

Melson, W. G., T. L. Vallier, T. L. Wright, G. Byerly, and J. Nelen (1976), Chemical diversity of abyssal volcanic glass erupted along Pacific, Atlantic, and Indian ocean sea-floor spreading centers, in *The Geophysics of the Pacific Ocean Basin and Its Margin*, *Geophys. Monogr. Ser.*, vol. 19, pp. 351–368, AGU, Washington, D. C.

Montelli, R., G. Nolet, F. A. Dahlen, G. Masters, E. R. Engdahl, and S.-H. Hung (2004), Finite-frequency tomography reveals a variety of plumes in the mantle, *Science*, *303*, 338–343.

Morgan, J. W., and E. Anders (1980), Chemical composition of Earth, Venus, and Mercury, *Proc. Natl. Acad. Sci. U. S. A.*, *77*, 6973–6977.

Morgan, J. W., R. J. Walker, A. D. Brandon, M. F. Horan, and E. Anders (2001), Siderophile elements in Earth's upper mantle and lunar breccias: data synthesis suggest manifestations of the same late influx, *Meteorit. Planet. Sci.*, *36*, 1257–1275.

Newsom, H. E., K. W. W. Sims, P. D. Noll, W. R. Jaeger, S. A. Maehr, and T. B. Beserra (1996), The depletion of tungsten in the bulk silicate Earth: Constraints on core formation, *Geochim. Cosmochim. Acta*, *60*, 1155–1169.

O'Neill, H. S. C. (1991), The origin of the Moon and the early history of the Earth—A chemical model: part 2. The Earth, *Geochim. Cosmochim. Acta*, *55*, 1150–1172.

O'Neill, H. S. C., and H. Palme (1998), Composition of the silicate Earth: Implications for accretion and core formation, in *The Earth's Mantle: Structure, Composition, and Evolution, The Ringwood Volume*, edited by I. Jackson, pp. 3–126, Cambridge Univ. Press, New York.

Palme, H., and A. Jones (2003), Solar system abundances of the elements, in *Treatise on Geochemistry*, vol. 1, edited by H. Holland and K. K. Turekian, pp. 41–61, Elsevier, New York.

Palme, H., and K. G. Nickel (1985), Ca/Al ratio and composition of the Earth's upper mantle, *Geochim. Cosmochim. Acta*, *49*, 2123–2132.

Palme, H., and H. S. C. O'Neill (2003), *Cosmochemical estimates of mantle composition, in Treatise on Geochemistry*, vol. 2, edited by H. Holland and K. K. Turekian, pp. 1–38, Elsevier, New York.

Ringwood, A. E. (1975), *Composition and Petrology of the Earth's Mantle*, McGraw-Hill, New York.

Saal, A. E., E. H. Hauri, C. H. Langmuir, and M. R. Perfit (2002), Vapour undersaturation in primitive mid-ocean-ridge basalt and the volatile content of Earth's upper mantle, *Nature*, *419*, 451–455.

Schilling, J.-G., M. B. Bergeron, R. Evans, and J. V. Smith (1980), Halogens in the mantle beneath the North Atlantic (and discussion), *Philos. Trans. R. Soc. London, Ser. A.*, *297*, 147–178.

Scott, E. R. D., and A. N. Krot (2003), Chondrites and their components, in *Treatise on Geochemistry*, vol. 3, edited by H. D. Holland and K. K. Turekian, pp. 143–200, Elsevier, New York.

Sims, K. W. W., H. E. Newsom, and E. S. Gladney (1990), Chemical fractionation during formation of the Earth's core and continental crust: Clues from As, Sb, W, and Mo, in *Origin of the Earth*, edited by H. E. Newsom and J. H. Jones, pp. 291–317, Oxford Univ. Press, New York.

Smith, J. V., J. S. Delaney, R. I. Hervig, and J. B. Dawson (1981), Storage of F and Cl in the upper mantle: Geochemical implications, *Lithos*, *14*, 133–147.

Stacey, J. S., and J. D. Kramers (1975), Approximation of terrestrial lead isotope evolution by two stage model, *Earth Planet. Sci. Lett.*, *26*, 207–211.

Sun, S.-S. (1982), Chemical composition and origin of the Earth's primitive mantle, *Geochim. Cosmochim. Acta.*, *46*, 179–192.

Takahashi, E. (1986), Melting of a dry peridotite KLB-1 up to 14 GPa: Implications on the origin of peridotitic upper mantle, *J. Geophys. Res.*, *91*, 9367–9382.

Turcotte, D. L., D. Paul, and W. M. White (2001), Thorium-uranium systematics require layered mantle convection, *J. Geophys. Res.*, *106*, 4265–4276.

van der Hilst, R. D., S. Widiyantoro, and E. R. Engdahl (1997), Evidence for deep mantle circulation from global tomography, *Nature*, *386*, 578–584.

Wade, J., and B. J. Wood (2001), The Earth's missing niobium may be in the core, *Nature*, *409*, 58–75.

Walter, M. J. (1998), Melting of garnet peridotite and the origin of komatiite and depleted lithosphere, *J. Petrol.*, *39*, 29–60.

Walter, M. J., and R. G. Trønnes (2004), Early Earth differentiation, *Earth Planet. Sci. Lett.*, *225*, 253–269.

Wänke, H. (1981), Constitution of terrestrial planets, *Philos. Trans. R. Soc. London, Ser. A*, *303*, 287–302.

Wänke, H., and G. Dreibus (1988), Chemical composition and accretion history of terrestrial planets, *Philos. Trans. R. Soc. London, Ser. A*, *325*, 545–557.

Wasserburg, G. J., G. J. F. MacDonald, F. Hoyle, and W. A. Fowler (1964), Relative contributions of uranium, thorium, and potassium to heat production in the Earth, *Science*, *142*, 465–467.

Wasson, J. T., and G. W. Kallemeyn (1988), Compositions of chondrites, *Philos. Trans. R. Soc. London, Ser. A*, *325*, 535–544.

Workman, R. K., and S. R. Hart (2005), Major and trace element composition of the depleted MORB mantle (DMM), *Earth Planet. Sci. Lett.*, *231*, 53–72.

Yi, W., A. N. Halliday, D.-C. Lee, and J. N. Christensen (1995), Indium and tin in basalts, sulfide and the mantle, *Geochim. Cosmochim. Acta*, *59*, 5081–5090.

Zhang, Y., and A. Zindler (1993), Distribution and evolution of carbon and nitrogen in Earth, *Earth Planet. Sci. Lett.*, *117*, 331–345.

————————————

J. Korenaga and T. Lyubetskaya, Department of Geology and Geophysics, P.O. Box, 208109, Yale University, New Haven, CT 06520-8109, USA. (jun.korenaga@yale.edu; tatiana.lyubetskaya@yale.edu)